Article

Molecular Cell

Proteasomal Control of Cytokinin Synthesis Protects *Mycobacterium tuberculosis* against Nitric Oxide

Graphical Abstract

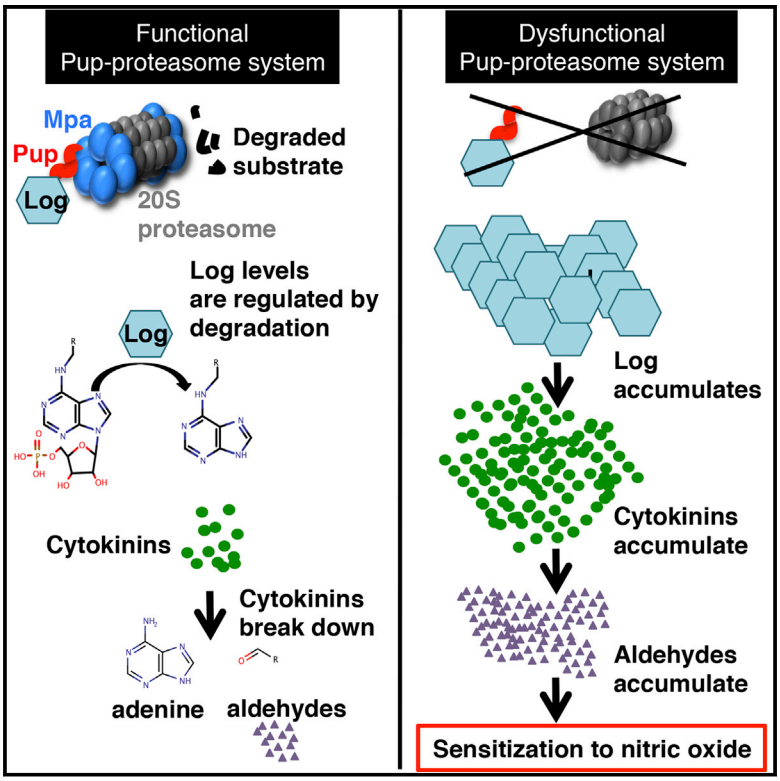

Highlights

- Accumulation of Rv1205 sensitizes *M. tuberculosis* to nitric oxide
- Rv1205 is a homolog of LONELY GUY, which makes cytokinins
- Cytokinin breakdown products synergize with NO to kill *M. tuberculosis*

Authors

Marie I. Samanovic, Shengjiang Tu, ..., Miroslav Strnad, K. Heran Darwin

Correspondence

heran.darwin@med.nyu.edu

In Brief

Samanovic et al. elucidated the link between proteasome function and NO resistance in *M. tuberculosis*. In a proteasome-defective strain, the accumulation of Rv1205, a homolog of a plant enzyme that synthesizes cytokinins, results in elevated cytokinin levels, the breakdown of which into aldehydes kills mycobacteria in the presence of NO.

Samanovic et al., 2015, Molecular Cell *57*, 984–994
March 19, 2015 ©2015 Elsevier Inc.
http://dx.doi.org/10.1016/j.molcel.2015.01.024

CellPress

Molecular Cell
Article

Proteasomal Control of Cytokinin Synthesis Protects *Mycobacterium tuberculosis* against Nitric Oxide

Marie I. Samanovic,[1] Shengjiang Tu,[2] Ondřej Novák,[3,4] Lakshminarayan M. Iyer,[5] Fiona E. McAllister,[6] L. Aravind,[5] Steven P. Gygi,[6] Stevan R. Hubbard,[7] Miroslav Strnad,[3,4] and K. Heran Darwin[1,*]

[1]Department of Microbiology, New York University School of Medicine, New York, NY 10016, USA
[2]Howard Hughes Medical Institute, Department of Biochemistry and Molecular Pharmacology, New York University School of Medicine, New York, NY 10016, USA
[3]Department of Metabolomics, Centre of the Region Haná for Biotechnological and Agricultural Research, Palacký University, 78371 Olomouc, Czech Republic
[4]Laboratory of Growth Regulators, Institute of Experimental Botany AS CR, 78371 Olomouc, Czech Republic
[5]National Center for Biotechnology Information, National Library of Medicine, NIH, Bethesda, MD 20894, USA
[6]Department of Cell Biology, Harvard Medical School, Boston, MA 02115, USA
[7]Department of Biochemistry and Molecular Pharmacology, The Skirball Institute, New York University School of Medicine, New York, NY 10016, USA
*Correspondence: heran.darwin@med.nyu.edu
http://dx.doi.org/10.1016/j.molcel.2015.01.024

SUMMARY

One of several roles of the *Mycobacterium tuberculosis* proteasome is to defend against host-produced nitric oxide (NO), a free radical that can damage numerous biological macromolecules. Mutations that inactivate proteasomal degradation in *Mycobacterium tuberculosis* result in bacteria that are hypersensitive to NO and attenuated for growth in vivo, but it was not known why. To elucidate the link between proteasome function, NO resistance, and pathogenesis, we screened for suppressors of NO hypersensitivity in a mycobacterial proteasome ATPase mutant and identified mutations in Rv1205. We determined that Rv1205 encodes a pupylated proteasome substrate. Rv1205 is a homolog of the plant enzyme LONELY GUY, which catalyzes the production of hormones called cytokinins. Remarkably, we report that an obligate human pathogen secretes several cytokinins. Finally, we determined that the Rv1205-dependent accumulation of cytokinin breakdown products is likely responsible for the sensitization of *Mycobacterium tuberculosis* proteasome-associated mutants to NO.

INTRODUCTION

Mycobacterium tuberculosis (*M. tuberculosis*) is one of the world's most devastating pathogens, killing nearly 1.5 million people yearly (http://www.who.int/mediacentre/factsheets/fs104/en/). Although many people are infected with this bacterium, most are able to suppress its growth, unless immunity wanes for reasons such as old age and immunosuppression due to HIV infection. *M. tuberculosis* resides in macrophages where the release of nitric oxide (NO) by the inducible NO synthase acts as a powerful anti-mycobacterial defense system (Chan et al., 1992, 1995; MacMicking et al., 1997). NO has the potential to damage nucleic acids, lipids, and proteins as well as displace metal co-factors from essential metabolic enzymes (reviewed in Bowman et al., 2011; Shiloh and Nathan, 2000). Despite the production of this important innate immune defense, *M. tuberculosis* remains an incredibly successful pathogen.

In order to understand how *M. tuberculosis* persists despite the macrophage production of NO, Carl Nathan's laboratory performed a screen for pathways that protect against NO-mediated toxicity and identified genes required for proteasome-dependent protein degradation in *M. tuberculosis* (Darwin et al., 2003). Proteasomes are barrel-shaped compartmentalized proteases that degrade proteins in a highly regulated manner (reviewed in Schmidt and Finley, 2014; Tomko and Hochstrasser, 2013). In eukaryotes, the best characterized substrates of the proteasome are post-translationally modified with the small protein ubiquitin (reviewed in Komander and Rape, 2012). In *M. tuberculosis,* most known substrates are modified with the small protein Pup (prokaryotic ubiquitin-like protein) (Pearce et al., 2008). Although functionally analogous to ubiquitylation, the biochemistry of pupylation is strikingly different. In *M. tuberculosis*, Pup is translated with a carboxyl-terminal glutamine that must be converted to glutamate by the enzyme Dop (deamidase of Pup) prior to substrate attachment by the only known Pup ligase PafA (proteasome accessory factor A) (Striebel et al., 2009). Pup then interacts with the hexameric ATPase Mpa (mycobacterial proteasome ATPase), which translocates doomed proteins into proteasome core proteases for degradation (Pearce et al., 2008; Striebel et al., 2009; Wang et al., 2010). In addition to the deamidation of Pup, Dop can also remove Pup from substrates prior to degradation (Burns et al., 2010; Cerda-Maira et al., 2010; Delley et al., 2012; Imkamp et al., 2010). Mutations in *dop*, *pafA*, *mpa* or the genes encoding

the *M. tuberculosis* 20S proteasome core protease (*prcBA*) sensitize bacteria to NO and attenuate bacterial growth in vivo, making the Pup-proteasome system (PPS) an attractive target for developing new tuberculosis therapeutics (Cerda-Maira et al., 2010; Darwin et al., 2003; Gandotra et al., 2007, 2010; Lamichhane et al., 2006; Lin et al., 2009). However, despite recent progress in characterizing the biochemistry of the mycobacterial PPS, the identification of the "pupylome" (Festa et al., 2010), and the transcriptional analysis of PPS mutants (Festa et al., 2011), the mechanism whereby proteolysis protects *M. tuberculosis* against NO stress had not been elucidated.

In this study, we performed an unbiased, genetic screen using an *mpa* null mutant to identify mutations that could suppress the NO-hypersensitivity phenotype of this strain. We found that disruption of Rv1205 suppressed the NO-sensitive phenotype of an *mpa* mutant. In addition, the Rv1205 mutation partially rescued the defective growth of the *mpa* mutant in mice. We found that Rv1205 is a Pup-proteasome substrate, the accumulation of which leads to NO sensitivity. We determined that Rv1205 is homologous to the plant enzyme LONELY GUY (LOG), which is a phosphoribohydrolase that catalyzes the final step in the production of cytokinins. Cytokinins are plant hormones that are crucial to the development of plants. Not only did Rv1205 have LOG activity, but we also found that *M. tuberculosis* secreted several cytokinins. Using an unbiased metabolomics analysis, we determined that the accumulation of cytokinin breakdown products was likely responsible for the sensitization of *M. tuberculosis* PPS mutants to NO. Thus, our data finally propose a mechanistic model for how proteasome activity can minimize the damaging effects of NO in *M. tuberculosis*.

RESULTS

A Suppressor Screen Identifies Mutations that Restore NO Resistance to a Proteasomal-Degradation-Deficient *M. tuberculosis* Strain

To elucidate the link between the PPS and NO resistance, we screened for genetic suppressors of the NO-hypersensitivity phenotype of a Δ*mpa::hyg* mutant. We made 18 ΦMycoMarT7 transposon (Sassetti et al., 2001) mutant pools, resulting in ~72,000 double mutants. Mutant pools were exposed to acidified nitrite, a source of NO, to enrich for NO-resistant clones. Three of the 18 pools yielded bacteria that survived two rounds of acidified nitrite exposure, and 360 clones were tested individually for NO resistance. After Southern blot analysis of 62 representative clones with increased NO resistance, we identified three allelic groups based on their BamHI restriction patterns (data not shown). We identified the transposon insertion sites (Figure 1A; Table S1) and quantified NO resistance of four representative mutants (Figure 1B). We complemented all of the suppressor mutations in single copy, resulting in the (re)sensitization of the mutants to NO (Figure 1B). An integrated plasmid encoding Rv1205 under the control of its native promoter complemented the *sup1* and *sup2* strains. Strain *sup3* had a mutation between the divergently expressed Rv2699c and Rv2700 genes and was complemented by Rv2700, but not Rv2699c. Rv2700 encodes a putative secreted protein with a predicted lipid-binding domain related to TraT, LytR, and CpsA (Pfam ID: PF03816) and is predicted to be essential for optimal growth in vitro (Sassetti et al., 2003); however, the *sup3* mutant grew normally under standard conditions (Figure 1C). Mutant *sup4* was complemented by *glpK*, which encodes a probable glycerol kinase and was the only mutant with a growth defect under normal culture conditions (Figure 1C). We also tested a strain with a transposon mutation in Rv1205 in an *mpa*$^{+}$ background; this strain exhibited wild-type (wt) NO resistance (Figure 1D), suggesting that disruption of Rv1205 alone does not cause NO hyperresistance under the conditions tested.

PPS-defective *M. tuberculosis* strains are highly attenuated in mice, partly due to their increased sensitivity to NO (Darwin et al., 2003). In addition to protecting against NO toxicity, the *M. tuberculosis* proteasome is required for the regulation of several metabolic pathways (Festa et al., 2010), including a copper homeostasis system that is essential for the full virulence of *M. tuberculosis* (Festa et al., 2011; Shi et al., 2014). Notwithstanding the pleiotropic role of Mpa and the proteasome in *M. tuberculosis* physiology, we tested if disruption of Rv1205 could reverse the attenuated phenotype of an *mpa* mutant in mice. We selected Rv1205 because it was identified twice in our screen and had a potentially interesting enzymatic activity that had not yet been described in *M. tuberculosis* (to be discussed later). We infected WT C57BL6/J mice by the aerosol inhalation route with WT, Δ*mpa::hyg*, Rv1205::ΦMycoMarT7, or *sup1* strains. The disruption mutation in Rv1205 partially restored the growth defect in the lungs and spleens of mice caused by the Δ*mpa::hyg* mutation (Figures 1E and 1F). The Rv1205 single mutant was as virulent as the WT strain at the observed time points, suggesting that Rv1205 activity is not required for virulence under the conditions tested. In one experiment, the Rv1205 mutant grew to higher numbers in the spleens compared to WT *M. tuberculosis*; however, this effect was not observed in both experiments.

Rv1205 Is a Newly Identified Pupylated Proteasome Substrate

At this point, we hypothesized that Rv1205 protein accumulated in the *mpa* mutant, resulting in NO sensitivity. We tested if Rv1205, or the other genes identified in the suppressor screen, encoded proteasome substrates. Rv1205, Rv2700, and *glpK* had not previously been identified to encode PPS substrates (Festa et al., 2010; Poulsen et al., 2010; Watrous et al., 2010), and none of these genes was differentially expressed in PPS mutants under routine culture conditions (Festa et al., 2011). We raised antibodies against hexahistidine-tagged Rv1205 and GlpK to determine if either accumulated in PPS-defective strains; attempts to produce recombinant Rv2700 have, so far, been unsuccessful. GlpK did not accumulate in mutants lacking the proteasome ATPase (*mpa*), the Pup ligase (*pafA*), or the proteasome core protease (*prcBA*) genes (Figure 2A). In contrast, Rv1205 accumulated in all three strains (Figure 2B). Rv1205 transcript levels were unchanged between the WT and *mpa* strains (Figure 2C), demonstrating that the accumulation of WT Rv1205 protein in the *mpa*, *pafA*, and *prcBA* mutants was likely due to failed degradation and not due to increased transcription of the Rv1205 gene. We pupylated Rv1205-His_6 in vitro and found that Pup modified lysine 74 (Figure 2D; Figure S1). Mutagenesis of lysine 74 to alanine

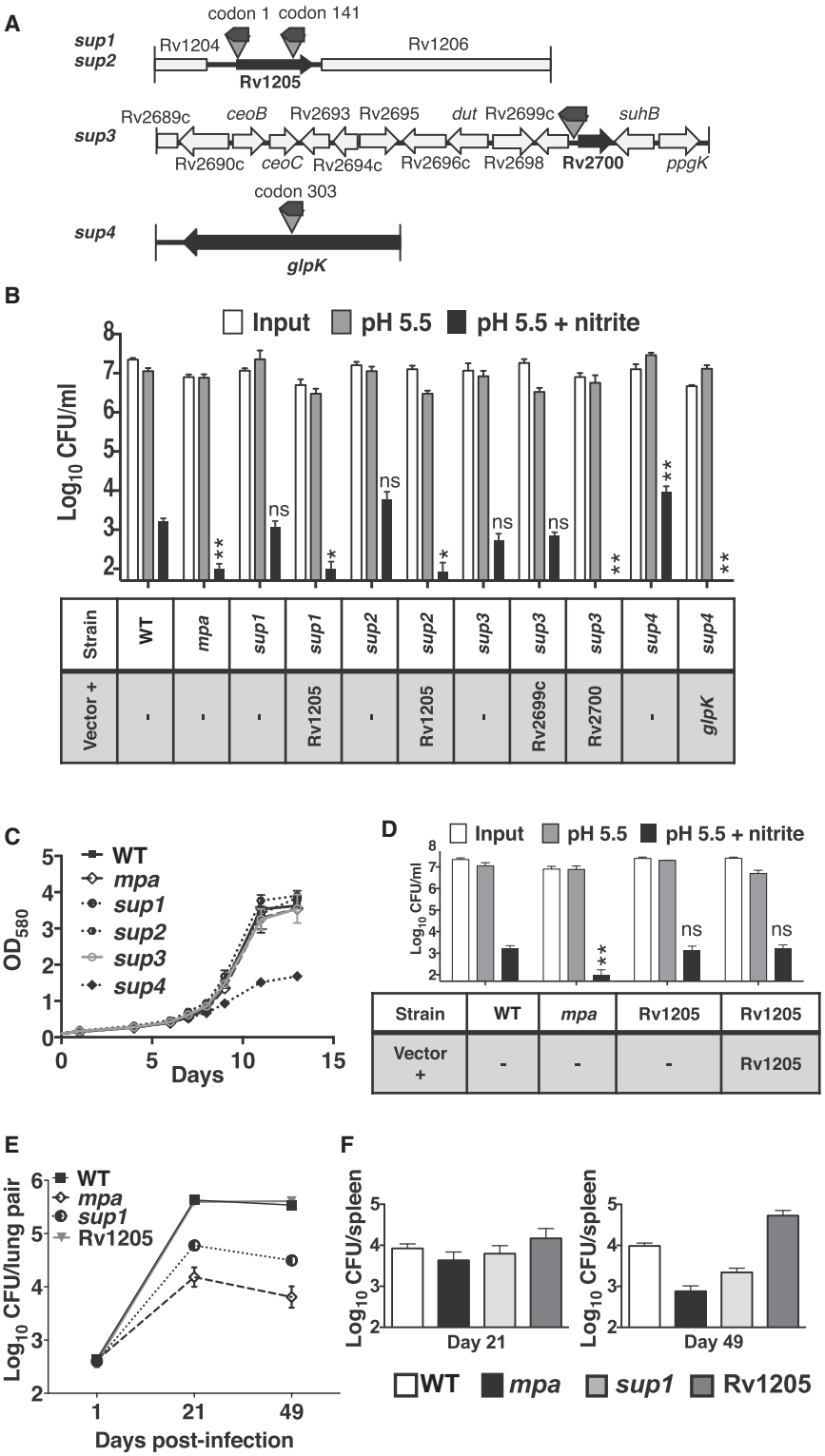

Figure 1. Identification of NO-Resistant Suppressor Mutants

(A) Genomic regions surrounding transposon insertions that suppressed the NO-sensitive phenotype of a Δ*mpa*::*hyg* mutant. Black arrows on triangles represent the direction of *neo* expression in the transposon. Gene data are from http://genolist.pasteur.fr/TubercuList/.

(B) NO susceptibility and complementation of suppressor mutants. All strains harbor an integrated pMV306.strep vector with or without the indicated gene. (–) indicates empty vector. Colony-forming units (CFU) of surviving bacteria after exposure to acidified media without (gray bars) or with (black bars) $NaNO_2$. Open bars show input CFU. Data show means ± SD, n = 3, from one of three independent experiments with similar results. All samples exposed to $NaNO_2$ were compared to WT with two-tailed Student's t test; *p < 0.05; **p < 0.01; ns, not statistically significantly different.

(C) Growth curves comparing WT, *mpa*, and *sup1-4* strains in 7H9 broth. Data show means ± SD, n = 3, from one of two independent experiments with similar results.

(D) NO susceptibility assay, as described in (B), of the Rv1205 mutant and the complemented strain. Data show means ± SD, n = 9, from three independent experiments. *p < 0.05; **p < 0.01; ns, not statistically significantly different.

(E and F) Disruption of Rv1205 partially restored virulence to an *mpa* mutant. Bacterial CFU after infection of WT C57BL6/J mice with WT, *mpa*, *sup1*, and Rv1205 strains. CFU from the lungs (E) and spleens (F) from two independent experiments at days 1 (n = 6), 21 (n = 8), and 49 (n = 8). Data show means ± SD. Data were analyzed for statistical significance by a two-way ANOVA followed by a Bonferroni posttest. For spleens: day 21, CFU were not significantly different; day 49, p < 0.05 between *mpa* and *sup1*. For lungs: day 21 and day 49, p < 0.001 and p < 0.01, respectively, between *mpa* and *sup1*.

($Rv1205_{K74A}$) abrogated Rv1205-His_6 pupylation in vitro (Figure 2D). Notably, $Rv1205_{K74A}$ accumulated in *M. tuberculosis* with a functional proteasome system (Figure 2E, far right). Thus, Rv1205 appears to be a substrate of the *M. tuberculosis* PPS.

Rv1205 Is a Homolog of the Plant Cytokinin-Activating Enzyme LOG

Rv1205 function had not been previously characterized but is annotated as a possible lysine decarboxylase (LDC) (Pfam ID: PF03641). However, we detected no LDC activity (L-lysine conversion to cadaverine) with Rv1205-His_6 under conditions in which *Escherichia coli* (*E. coli*) LDC was strongly active (data not shown). However, using sequence profile searches with the PSI-BLAST and JACKHMMER programs, we established that Rv1205 is related to the rice *Oryza sativa* protein LOG (e value = 10^{-24} in iteration 2), an enzyme that catalyzes the hydrolytic removal of ribose 5′-monophosphate from nitrogen (N^6)-modified adenosines, the final step of bioactive cytokinin synthesis (Figure 3A) (Kurakawa et al.,

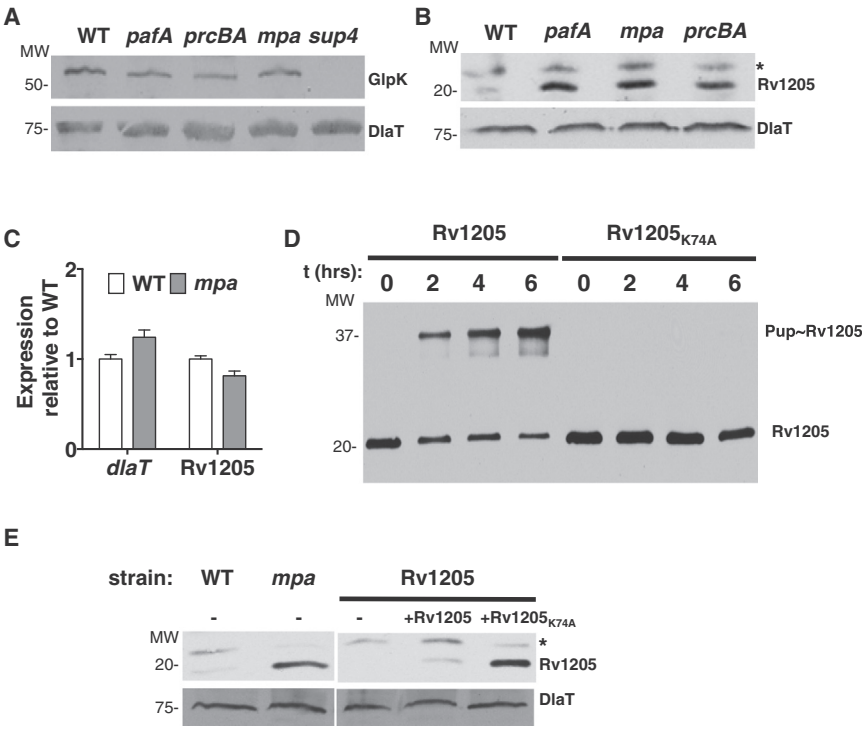

Figure 2. Rv1205 Is a Newly Identified Proteasome Substrate

(A) Immunoblot for GlpK in total cell lysates of WT, *prcBA*, *pafA*, *mpa,* and *sup4* strains. MW, molecular weight.

(B) Immunoblot for Rv1205 (20 kD) in total cell lysates of WT, *mpa*, *pafA*, and *prcBA* strains.

(C) Quantitative real-time PCR shows that Rv1205 transcripts were unchanged in the *mpa* mutant when compared with WT *M. tuberculosis*. Fold changes relative to WT *M. tuberculosis* are plotted on the y axis. This experiment represents one biological replicate performed in triplicate. Data indicate means ± SD. *dlaT* (dihydrolipoamide acyltransferase) was used as a control for a gene whose expression does not change in PPS mutants.

(D) In vitro pupylation assay of recombinant histidine-tagged Rv1205 and $Rv1205_{K74A}$. Proteins were detected with polyclonal antibodies to Rv1205-His_6.

(E) Immunoblot for Rv1205 in total cell lysates of WT, *mpa*, and Rv1205 strains harboring integrated vector with or without the Rv1205 gene. −, empty vector. The loading control for all immunoblots is DlaT. For all panels, the MW markers are indicated on the left. The asterisk represents a cross-reactive protein in (B) and (E).

See also Figure S1.

2007). Furthermore, these searches, as well as profile-profile comparisons with HHpred (Söding et al., 2005), revealed no significant relationship between LOG family members and the LDC superfamily. The crystal structure of the Rv1205 ortholog in the close *M. tuberculosis* relative *Mycobacterium marinum* (*M. marinum*) was previously crystallized (Protein Data Bank [PDB] ID: 3SBX) in an effort by the Seattle Structural Genomics Center for Infectious Disease to characterize mycobacterial proteins of unknown function. HHpred analysis revealed that this protein, MMAR_4233, looks virtually identical to *Arabidopsis thaliana* (*A. thaliana*) LOG (Figure 3B).

Cytokinins are hormones that are critical for plant development (reviewed in Argueso et al., 2009) and are also produced by bacterial phytopathogens and phytosymbionts to promote their growth in plants (reviewed in Frébort et al., 2011). Cytokinins are adenine derivatives that usually have either an isoprene-derived or an aromatic side chain at the N^6 position. In plants, isoprenoid cytokinins—N^6-(Δ^2-isopentenyl) adenine or isopentenyladenine (iP); *trans*-zeatin (*t*Z); *cis*-zeatin (cZ), and dihydrozeatin (DHZ)—are more typically observed and found in greater abundance than aromatic cytokinins (*meta*-, *ortho*-, and *para*-topolins) (reviewed in Sakakibara, 2006). For cytokinin synthesis, two pathways have been described: the direct de novo biosynthesis of free cytokinins (prenylated adenylic nucleotides) and the salvage of cytokinins from tRNAs, which typically have prenyl modifications (reviewed in Kamada-Nobusada and Sakakibara, 2009).

Some phytobacteria deploy cytokinins synthesized by dedicated operons, which include a LOG-like gene, against their plant hosts. We observed LOG homologs in all major lineages of prokaryotes (Figure 3C; Figure S2), but not in species such as *E. coli* and most obligate intracellular pathogens with reduced genomes. Several Actinobacteria, but not *Mycobacteria*, contain two adjacent LOG-like genes. The presence of LOG-like genes often correlates with the presence of *miaA,* a gene involved in the prenylation of a highly conserved adenine at the 3′ end of tRNA anticodons that facilitates translational fidelity (Bjork, 1996; Urbonavicius et al., 2001). LOG-like genes can also be found in operons with *mazG* in several bacterial species (e.g., *M. marinum*). MazG proteins, which have pyrophosphatase activity, could potentially hydrolyze N^6-prenylated ATP to generate N^6-prenylated AMP, a LOG-like enzyme substrate. In some species, LOG domains are fused to a MutT/Nudix-type hydrolase, which could also possibly catalyze pyrophosphate hydrolysis of nucleotide triphosphates to create LOG substrates (McLennan, 2006).

Rv1205 Is a Phosphoribohydrolase that Produces Cytokinins

We next determined if *M. tuberculosis* produced cytokinins, an activity that had never been reported before in a mammalian pathogen or symbiont. Using a mass-spectrophotometric protocol developed specifically for the analysis of plant cytokinins, we quantified several cytokinins and their derivatives in the supernatants and cellular extracts of *M. tuberculosis* cultures (Figure S3; Table 1; Table S2). iP and 2-methylthio-iP (2MeS-iP) were the most abundant cytokinins detected in *M. tuberculosis* lysates and supernatants (Figure S3; Table 1, cytokinins are indicated with a subscript a). It is important to note that we observed a significant accumulation of 2MeS-iP in the *mpa* mutant supernatants with a concomitant reduction of the dephosphorylated form (2MeS-isopentenyladenosine [2MeS-iPR]) of its presumed

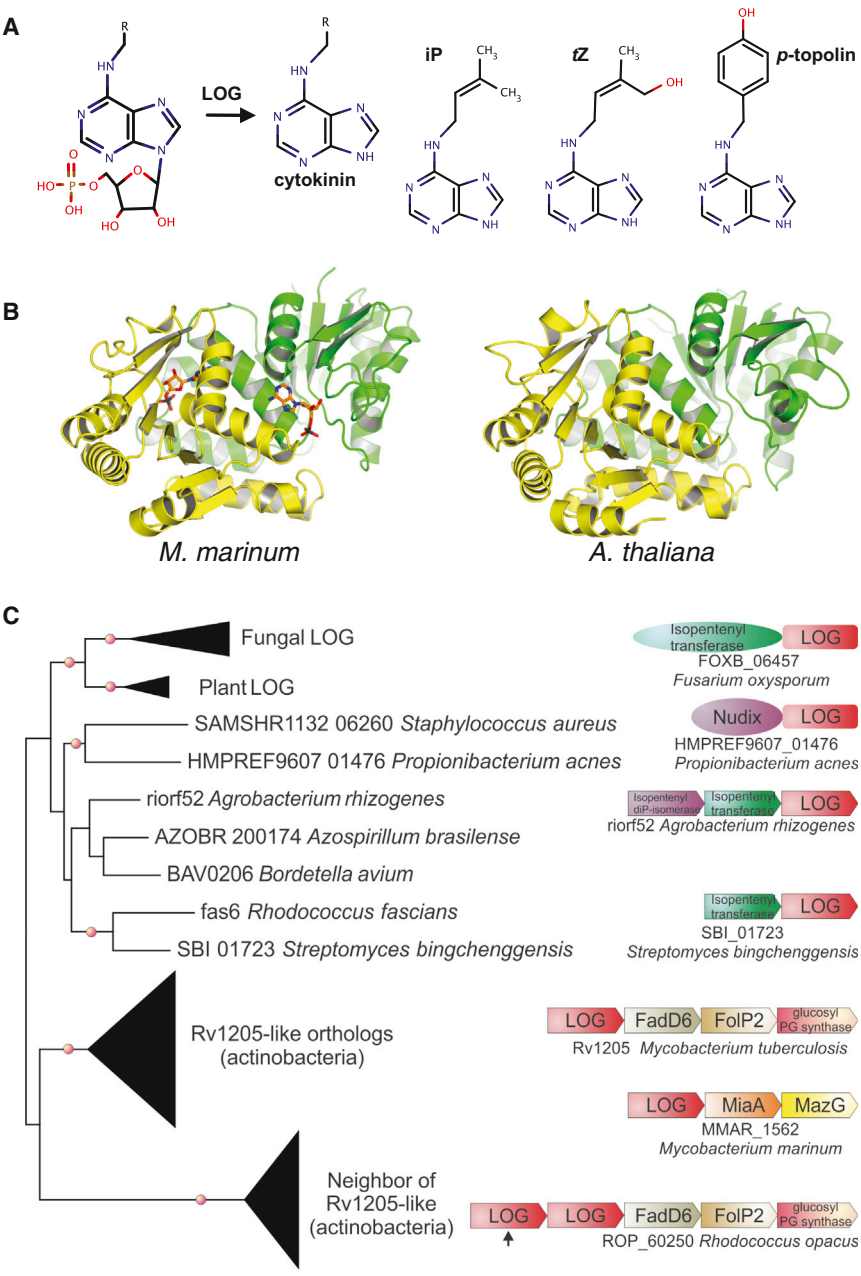

Figure 3. Rv1205 Is a Homolog of LOG

(A) LOG activity and structures of select cytokinins. R, isoprene-derived or aromatic side chain.

(B) Comparison of the crystal structures of proteins from *M. marinum* (left; PDB ID: 3SBX) and *A. thaliana* (right; PDB ID: 1YDH). The two subunits in the homodimers are green and yellow. AMP molecules in the *M. marinum* structure are shown in stick representation with carbon atoms in orange, oxygen atoms in red, nitrogen atoms in blue, and phosphorus atoms in black.

(C) Phylogenetic analysis of LOG-like genes. Clades with bootstrap values greater than 90% have a red circle. Well-supported monophyletic clades are shown as filled triangles. Predicted operons and domain architectures are illustrated to the right. Names of the LOG-like genes are indicated below.

See also Figure S2.

precursor (2MeS-isopentenyladenosine monophosphate [2MeS-iPRMP]) in the cell pellet (Table 1). These results were consistent with the notion that the *mpa* mutant had more Rv1205 protein and, thus, more LOG-like activity. It is notable that the cytokinin ribosides (iPR and 2MeS-iPR) were more apparent than the nucleotides (iPRMP or 2MeS-iPRMP, which was undetectable). Although the nucleotide forms (Table 1, indicated with a subscript b) are substrates of LOG-like enzymes, we believe that these are rapidly dephosphorylated into the riboside forms; therefore, both nucleosides and nucleotides could be considered cytokinin precursors. Thus, when one considers both the phosphorylated and unphosphorylated ribosides in total, it is apparent that these are reduced in the *mpa* mutant. We did not observe accumulation of the cytokinin iP in the *mpa* strain samples as we would have expected; however, iP may possibly be turned over upon accumulation or rapidly modified to make 2MeS-iP, which accumulates in the *mpa* strain as one might expect.

As expected with strains lacking Rv1205, we observed a significant reduction in the amount of several cytokinins. iP levels were almost 30 times lower in the *sup1* and Rv1205 mutant supernatants, along with a corresponding increase in the concentration of the cytokinin precursors (e.g., iPRMP increased in the Rv1205 mutants almost 10-fold in cell lysates). Remarkably, the level of 2MeS-iP was reduced by almost two orders of magnitude in strains lacking Rv1205. It was notable that *tZ*, *cZ*, DHZ, and their derivatives, which are important cytokinins in the plants, did not follow Rv1205 protein levels, in contrast to iP and 2MeS-iP, which suggests possible alternative pathways for the biosynthesis of these cytokinins in *M. tuberculosis*.

Using a high-performance liquid chromatography (HPLC)-based assay, we tested Rv1205-His_6 for LOG activity and found that it hydrolyzed two different commercially available cytokinin nucleoside monophosphates: iP and *tZ* (Figure 4A). Rv1205 had a Michaelis-Menten constant (K_M) of 5.6 μM, a catalytic rate constant (k_{cat}) of 434.3 min^{-1}, and a k_{cat}/K_M ratio of 7.8 × 10^7 $min^{-1}M^{-1}$ for iPRMP (Figure 4B). As controls, Rv1205 did not hydrolyze ATP (Figure 4A) and hydrolyzed AMP slowly: K_M = 73.1 μM, k_{cat} = 2.3 min^{-1}, and k_{cat}/K_M = 3.1 × 10^4 $min^{-1}M^{-1}$, suggesting that neither was a natural substrate of this enzyme (Figure 4C).

Based on the crystal structure of the *M. marinum* protein, we mutated several conserved residues in Rv1205 that were

Table 1. Quantification of Cytokinins in *M. tuberculosis*

	WT	*mpa*	*sup1*	Rv1205	*sup1* + $Rv1205_{D120A,E121A}$
Lysates					
iP[a]	121.09 ± 21.88	89.66 ± 6.75	30.17 ± 4.01**	27.11 ± 3.33**	21.65 ± 1.23**
iPR	125.81 ± 7.55	39.12 ± 8.23***	822.85 ± 177.87**	983.59 ± 169.25**	352.49 ± 76.72*
iPRMP[b]	298.74 ± 49.81	185.72 ± 18.68*	3,595.85 ± 640.44**	2,021.84 ± 319.05**	1,750.04 ± 379.28**
2MeS-iP[a]	11,916.7 ± 1,620.4	12,130.6 ± 1,091.8	183.7 ± 59.1***	141.5 ± 38.6***	222.8 ± 75.0***
2MeS-iPR	19,895.9 ± 2,441.2	8,164.8 ± 195.8**	29,614.2 ± 5,138.7	40,724.0 ± 6,622.2*	29,187.0 ± 2,727.8*
tZ[a]	1.33 ± 0.24	1.23 ± 0.19	0.65 ± 0.17*	3.60 ± 0.91*	2.48 ± 0.24**
tZR	0.71 ± 0.16	0.95 ± 0.19	0.92 ± 0.10	1.56 ± 0.31*	0.79 ± 0.05
2MeS-*tZR*	49.28 ± 10.46	89.20 ± 30.49	58.69 ± 15.89	33.72 ± 11.48	55.01 ± 4.27
Media					
iP[a]	234.39 ± 18.03	258.44 ± 36.17	7.8 ± 1.7***	–	10.57 ± 1.49***
iPR	47.52 ± 5.65	10.92 ± 1.00***	121.10 ± 20.06**	–	260.18 ± 24.66***
iPRMP[b]	11.15 ± 1.17	9.29 ± 0.27	10.05 ± 0.31	–	6.59 ± 0.46**
2MeS-iP[a]	6,184.89 ± 191.77	10,293.56 ± 1,441.70*	61.4 ± 15.8***	–	17.51 ± 0.55***
2MeS-iPR	5,830.93 ± 141.05	3,013.1 ± 523.0**	10,243.2 ± 1,671.2*	–	12,354.6 ± 1,616.2**
tZ[a]	0.16 ± 0.04	0.145 ± 0.038	0.015 ± 0.003**	–	0.029 ± 0.004**
tZR	1.36 ± 0.30	1.677 ± 0.356	1.758 ± 0.450	–	<LOD
2MeS-*tZR*	86.19 ± 6.08	40.175 ± 4.706**	132.855 ± 17.364*	–	54.042 ± 15.142*

Cytokinin and cytokinin precursor levels in the supernatants of *M. tuberculosis* culture (Media) and in 1 g (wet weight) of cells (Lysate) grown to an OD_{580} of 1. Ribosides are likely dephosphorylated LOG-like substrates. Values are in picomoles per liter; mean ± SD, n = 3. Asterisks indicate statistically significant difference in mutant lines versus WT with an ANOVA (*$p < 0.05$, **$p < 0.01$, and ***$p < 0.001$). LOD, limit of detection, defined as a signal-to-noise ratio of 3:1. *tZR*, *trans*-zeatin-riboside; 2MeS-*tZR*: 2-methylthio-*trans*-zeatin-riboside. See also Figure S3 and Table S2.

[a]Cytokinins.

[b]LOG-like enzyme substrates.

predicted to coordinate or hydrolyze cytokinin precursors and tested the activity of the mutant proteins (Figure 4D). Although we cannot definitively be certain that the proteins were properly folded, all five mutant proteins were as soluble as the WT protein dimer, and each migrated similarly to WT Rv1205 in native gels (Figure 4E). Mutagenesis of the conserved residues significantly reduced phosphoribohydrolase activity (Figure 4F; Figure S4). Additionally, Rv1205 with mutations at aspartate 120 and glutamate 121 (D120A E121A) failed to restore cytokinin secretion in the *mpa* Rv1205 (*sup1*) mutant (Table 1). Based on the strong conservation among different species, we predict that glutamate 121 is a key catalytic residue of Rv1205 (Figure 4D).

We also performed NO-susceptibility assays on the *sup1* strain transformed with the mutant Rv1205 alleles and found that the *mpa* mutant sensitivity to NO was linked to functional Rv1205 activity (Figure 5).

In Figure 2B, we showed that Rv1205 accumulated in PPS mutants and mutagenesis of Rv1205 Lys74 to Ala resulted in stabilization of the protein (Figure 2E). We tested the NO-susceptibility of this strain and found that it was significantly more sensitive to NO than WT bacteria but not as sensitive as an *mpa* strain (Figure S5A). We measured phosphoribohydrolase activity of $Rv1205_{K74A}$ and found that this protein had drastically reduced activity (Figure S5B), possibly explaining the lack of a robust NO-sensitization phenotype. We also tried to overproduce Rv1205 in WT bacteria with the overexpression plasmid pOLYG (Garbe et al., 1994); however, this was toxic to the bacteria, and we could not use this strain in an NO assay (data not shown).

Because Rv1205 is a cytokinin-producing phosphoribohydrolase that is highly similar to plant LOG, we hereinafter refer to Rv1205 and its mycobacterial orthologs as "Log."

Accumulation of Aldehydes Leads to NO Sensitivity

To gain some understanding of the impact of increased cytokinin levels in the *mpa* mutant, we examined the metabolites present in cell extracts of the WT, *mpa*, *sup1* (*mpa log*), and *log* strains. We used a global screening approach and detected a total of 220 metabolites (155 compounds of known identity and 65 compounds of unknown structural identity), and we examined metabolites that differed significantly between experimental groups (see Table S3 for statistical summary). The strongest observed change in the *mpa* strain relative to the WT strain was the accumulation of *para*-hydroxybenzaldehyde (*p*HBA) (Figure 6A; Table S4). pHBA can form via several pathways, including the enzymatic degradation of the aromatic cytokinin *para*-topolin (*p*-topolin) by cytokinin oxidases (Popelková et al., 2006). Aromatic cytokinins (*meta*-, *ortho*-, and *p*-topolins) and their precursors were also detected in our *M. tuberculosis* lysates and supernatants analysis, but with levels near the limit of detection of our assay (data not shown). Using a spectrophotometric assay for the detection of aldehyde formation, we detected conversion of exogenously added *p*-topolin into pHBA in *M. tuberculosis* cell extracts, suggesting that cytokinin oxidase activity is present in *M. tuberculosis* (Figure 6B).

In addition to pHBA, we observed a significant accumulation of several fatty acids (linoleate, palmitoleate, margarate, and

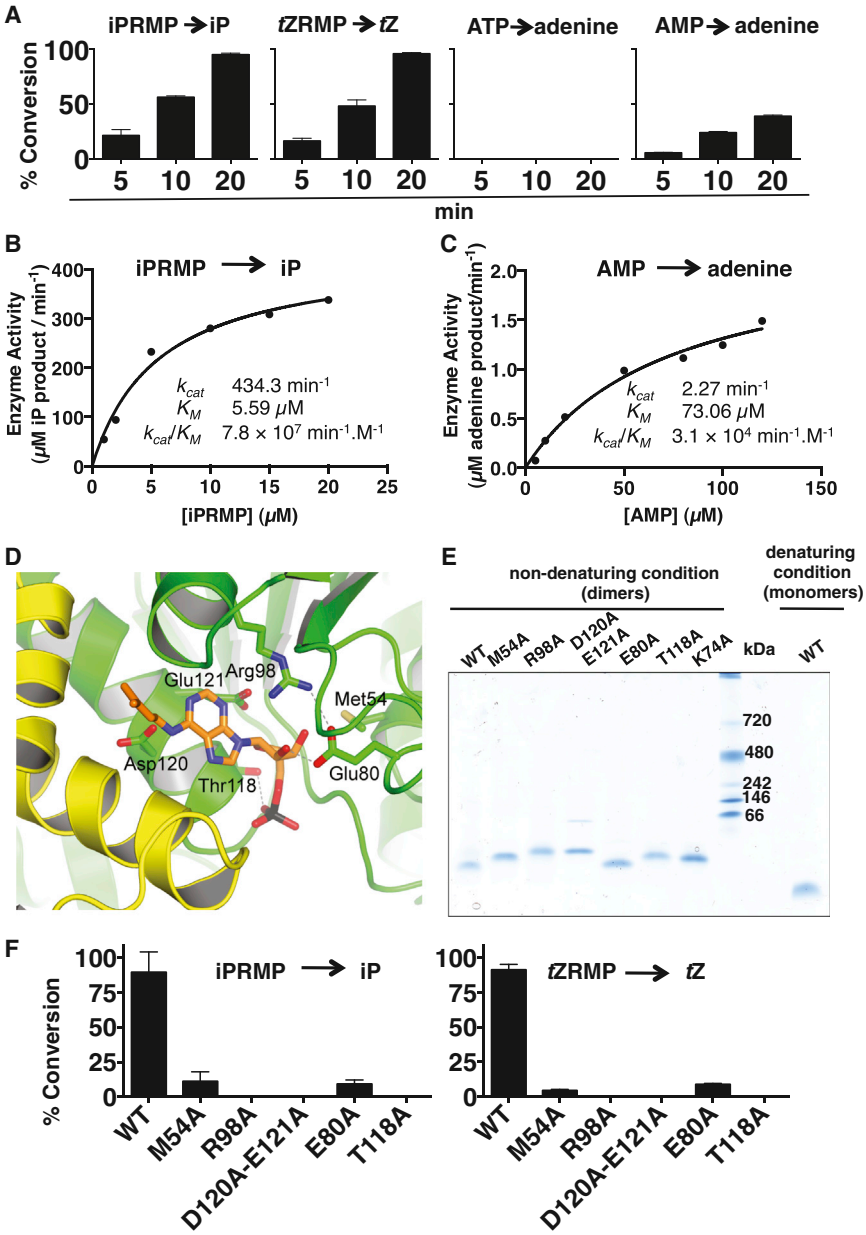

Figure 4. Rv1205 Is a Phosphoribohydrolase

(A) Rv1205-His_6 phosphoribohydrolase activity toward the substrates iPRMP and *t*Z-riboside monophosphate (*t*ZRMP) as measured by HPLC (error bars indicate means ± SD, n = 3). ATP and AMP were used as controls.

(B and C) Determination of Rv1205 kinetic parameters for iPRMP (B) and AMP (C) conversion to iP and adenine, respectively.

(D) Three-dimensional model of Rv1205 constructed using SWISS-MODEL (Arnold et al., 2006) based on *M. marinum* (PDB ID: 3SBX), which has a sequence identity of 84% to Rv1205. The viewing angle is the same as in Figure 3B. The ribbon diagram is centered on the presumed active site, with iPRMP placed according to the position of AMP in the *M. marinum* structure. Rv1205 is predicted to be a homodimer (subunits are in green and yellow). Selected side chains are shown in stick representation. Atom colors: carbon in Rv1205 (green) or iPRMP (orange), oxygen (red), nitrogen (blue), sulfur (yellow), and phosphorus in iPRMP (black). Dotted lines indicate potential hydrogen bonding.

(E) Separation by native gel electrophoresis of recombinant WT or mutant Rv1205-His_6 proteins.

(F) Activity of point mutant alleles of Rv1205-His_6 with indicated substrates. Data show means ± SD, n = 3.

See also Figure S4.

oleate) and lipid peroxidation products (9-hydroxy-10,12-octadecadienoic acid [9-HODE] and 13-hydroxy-9,11-octadecadienoic acid [13-HODE]) in the *mpa* mutant (Figure 6A). Disruption of *log* in the *mpa* mutant (*sup1*) restored WT levels of all of these metabolites as well as pHBA.

We next tested if exogenously added pHBA could kill *M. tuberculosis* in the presence or absence of NO. We found that, in a dose-dependent manner, micromolar concentrations of pHBA dramatically killed WT *M. tuberculosis* in acidified nitrite but not in acidic media alone or acidified nitrate (Figure 6C; Figure S6). Increased nitrite sensitivity due to pHBA was also observed for *M. smegmatis* but not for *E. coli* (Figure S6).

The breakdown of all cytokinins results in the appearance of adenine and an aldehyde derived from the N^6 position of the adenine base (Frébort et al., 2011). Metabolomics analysis did not reveal aldehydes other than pHBA; however, the other aldehydes of cytokinin degradation are highly unstable. iP and 2MeS-iP were among the most abundant cytokinins observed in *M. tuberculosis* culture supernatants; therefore, we tested if the aldehyde breakdown product of these two molecules, 2-methyl-3-butenal, could sensitize *M. tuberculosis* to NO. While 2-methyl-3-butenal was highly volatile, it could nonetheless exacerbate killing of *M. tuberculosis* by NO (Figure 6D). Thus, it appears that at least two different cytokinin breakdown products could synergize with NO to kill *M. tuberculosis*.

DISCUSSION

In this work, we determined how the PPS protects *M. tuberculosis* against NO by an unbiased, genetic approach. We identified four independent mutants, two with insertions in Rv1205 or *log*. We showed that disruption of *log* in a proteasome-defective strain not only restored NO resistance to WT levels but also restored a significant amount of bacterial growth in mice. We further established that Log is a pupylated proteasome substrate that accumulates in proteasome degradation-defective strains. Log has high structural similarity to the plant enzyme LOG and has the

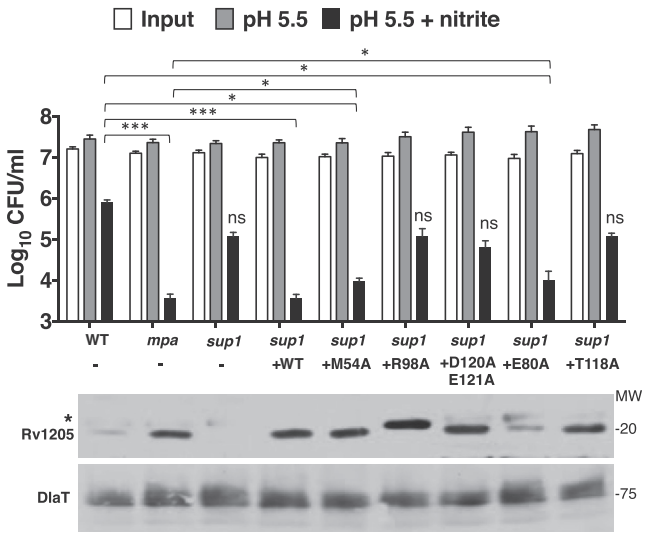

Figure 5. Site-Directed Mutagenesis of Rv1205 Abrogates NO Sensitization in *M. tuberculosis*

Point mutant alleles of Rv1205 could not fully restore NO sensitivity to the *sup1* mutant. Data show means ± SD, n = 9 (upper panel). All samples exposed to $NaNO_2$ were compared to WT with a two-tailed Student's t test. *p < 0.05; ***p < 0.001; ns, not statistically significantly different. Samples showing statistical difference to WT were also compared to *mpa*, and significant differences are similarly indicated; these data suggest partial complementation. Immunoblot for Rv1205 (20 kD) in total cell lysates of indicated strains. DlaT is the loading control. Molecular weight (MW) markers are indicated on the right. The asterisk represents a cross-reactive protein. CFU, colony-forming units; A, alanine; M, methionine; R, arginine; D, aspartate; E, glutamate; T, threonine. See also Figure S5.

same phosphoribohydrolase activity as plant LOGs, which convert N^6-modified AMP derivatives into cytokinin free bases. Using metabolomics, we found the accumulation of at least one cytokinin breakdown product, pHBA, in an *mpa* mutant. We determined that pHBA and another aldehyde product of cytokinin metabolism synergize with NO to kill *M. tuberculosis*. Aldehydes are known to target membranes (Schauenstein et al., 1977), which might explain the lipid peroxidation observed in our metabolomics analysis. Furthermore, NO and other reactive nitrogen intermediates could possibly exacerbate this process. Although we cannot rule out that the accumulation of active Log has additional effects that result in NO sensitivity, our data currently support a model where the accumulation of aldehydes likely contributes to the NO-hypersusceptibility phenotype of PPS mutants. Thus, our work suggests that the accumulation of a single protein, rather than bulk protein damage, is sufficient to sensitize proteasome-defective *M. tuberculosis* to NO. Notably, this work demonstrates that a mammalian bacterial pathogen produces cytokinins. This observation is remarkable when one considers that *M. tuberculosis* is never found in an environmental reservoir where it could encounter plants.

The *M. tuberculosis* proteasome was discovered in an effort to understand how this human-exclusive pathogen persists in the face of a robust immune response, which includes the production of NO. Although several groups purified and identified pupylated proteins in *M. tuberculosis* and *M. smegmatis* (Festa et al., 2010; Poulsen et al., 2010; Watrous et al., 2010), none of the studies was able to link a particular proteasome substrate to NO resistance. Incredibly, none of the proteomics approaches identified Log, presumably because, under normal conditions, Log must be kept at very low levels, as evidenced in our immunoblots, where we could barely detect endogenous Log in WT *M. tuberculosis* (Figures 2B and 2E).

A *log* homolog was previously detected in a screen for *M. marinum* genes specifically expressed in the granulomas of infected frogs but not in cultured macrophages (Ramakrishnan et al., 2000). This suggests that Log has a role during specific phases of mycobacterial infections that have yet to be determined. Another small adenosine-derived molecule (1-tuberculosinyladenosine, or 1-TbAd) was recently discovered in *M. tuberculosis* with a probable involvement in virulence (Layre et al., 2014). However, to date, there are no data suggesting that 1-TbAd is linked to cytokinin biosynthesis, and 1-TbAd levels were similar among our strains (Table S4).

The function of cytokinins in *M. tuberculosis* is unknown. In plants, cytokinins regulate numerous developmental processes and responses to the environment (Sakakibara, 2006) as well as promote defense against pathogens (Choi et al., 2011). Conversely, cytokinin production allows several phytopathogens to redirect plant development and nutrient distribution to facilitate microbial growth. The actinomycete *Rhodococcus fascians*, a distant relative of *M. tuberculosis*, induces plant pathology via the local and persistent secretion of cytokinins (Pertry et al., 2009). Why would *M. tuberculosis,* a human-adapted pathogen, produce cytokinins? We speculate that cytokinins may be used as signaling molecules to communicate among mycobacteria and/or have an impact on the host to help bacteria establish a successful infection.

Finally, it is notable that *M. tuberculosis* produces Log and tightly controls its levels post-translationally, supporting the notion that the untimely presence of Log is detrimental for the lifestyle of this pathogen. Other bacterial species—in particular, important animal pathogens like *Staphylococcus aureus* and *Bordetella* species—harbor LOG homologs (Figure 3C). Therefore, it will be interesting to determine the function of what were once believed to be plant-exclusive hormones in other bacterial systems and their animal hosts.

EXPERIMENTAL PROCEDURES

Details of experimental procedures are described in the Supplemental Experimental Procedures.

Bacterial Strains, Plasmids, Primers, Chemicals, and Culture Conditions

Bacterial strains, plasmids, and primer sequences used in this study are listed in Table S1. See Supplemental Experimental Procedures for details.

iPRMP, *t*ZRMP, iP, *t*Z, and *p*-topolin were purchased from OlChemim. pHBA and 2-methyl-3-butenal were purchased from Sigma.

Transposon Mutagenesis, Nitrite Treatment, and Suppressor Screen

We mutagenized Δ*mpa*::*hyg* mutant cultures with the mariner-based ΦMycoMarT7 transposon (Kan^R) (Sassetti et al., 2001). We generated 18 independent pools with ~4,000 double mutants per pool (Hyg^R, Kan^R). Each pool was then exposed for 6 days to 3 mM $NaNO_2$ in 7H9 at pH 5.5. Bacteria were allowed to

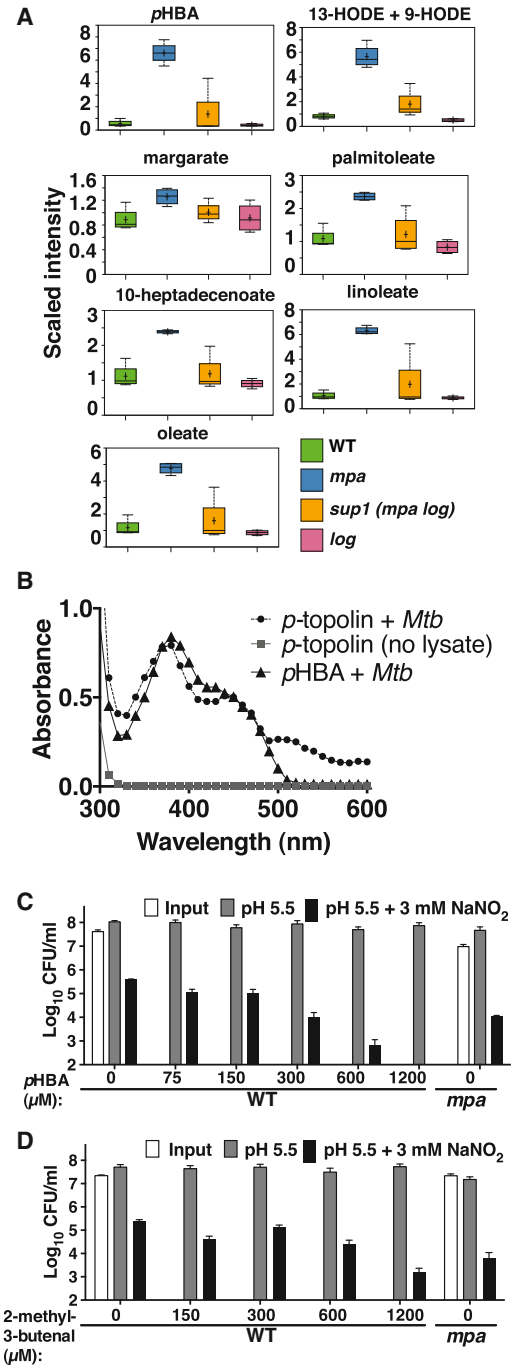

Figure 6. Aldehyde Accumulation in *M. tuberculosis* Causes NO Sensitivity

(A) Metabolomics analysis revealed several molecules at elevated levels in an *mpa* mutant. Results of relevant compounds from cell lysates of WT, *mpa*, *sup1*, and *log M. tuberculosis* strains (n = 4).

(B) Detection of pHBA, a degradation product of *p*-topolin, in *M. tuberculosis* lysates. Absorption spectra of the 4-aminophenol assay, which detects aldehyde release, are shown. *p*-topolin without *M. tuberculosis* lysate (■), 500 μM *p*-topolin with *M. tuberculosis* lysate (●), and 300 μM pHBA with *M. tuberculosis* lysate (▲) was used as a positive pHBA control. *M. tuberculosis* lysate was used as a blank for the latter two experiments.

(C) pHBA sensitized WT *M. tuberculosis* to NO in a dose-responsive manner. Data show means ± SD, n = 3.

(D) 2-methyl-3-butanal sensitized WT *M. tuberculosis* to NO in a dose-responsive manner. Data show means ± SD, n = 3.

See also Figure S6 and Tables S3 and S4.

recover in 7H9 medium at pH 6.8 until bacterial growth was observed, about 3–5 weeks, depending on the pool. Three pools recovered and were subjected to another round of acidified nitrite treatment for 6 days and directly plated on 7H11 agar.

A total of 120 individual colonies were picked from each of the three pools and inoculated into 200 μl 7H9 until growth reached stationary phase. Ten microliter aliquots of each mini-culture were then sub-cultured into 190 μl of acidified 7H9 containing a final concentration of 3 mM $NaNO_2$. After 6 days, 50 μl from each well was mixed with 150 μl 7H9 (pH 6.8), and recovery was monitored by optical density at 580 nm (OD_{580}) 2–3 weeks later. Double mutant recovery was compared to the recovery of WT (NO-resistant) and Δ*mpa*::*hyg* (NO-sensitive) strains undergoing the same treatment. Candidate suppressor mutants were selected if the OD_{580} was comparable to the WT control.

Sixty-two clones were selected through this protocol (24, 24, and 14 from pools 4, 6, and 12, respectively). Chromosomal DNA from all 62 was analyzed by Southern blotting (data not shown). See Supplemental Experimental Procedures for details.

Each mutant had a single, unique transposon insertion. We detected three different restriction patterns from the mutants and surmised that three different loci were affected. One pattern was found in two pools (4 and 6). Genomic DNA encompassing the transposon insertion site was cloned and sequenced as previously described (Darwin et al., 2003). DNA sequencing using a primer that annealed to the *neo* gene was performed by GENEWIZ.

Nitrite resistance was quantified by NO assay for each of the suppressor mutants exactly as described previously (Darwin et al., 2003).

Mouse Infections

Mouse infections were performed essentially as described previously (Darwin et al., 2003). All procedures were performed with the approval of the New York University Institutional Animal Care and Use Committee. See Supplemental Experimental Procedures for details.

Protein Purification and Immunoblotting

Recombinant protein production and immunoblotting analysis of *M. tuberculosis* cell lysates was performed essentially as previously described (Festa et al., 2007). See Supplemental Experimental Procedures for details.

In Vitro Pupylation Assay

In vitro conjugation of Pup_{Glu} (10 μM) to Log (2 μM) was carried out at room temperature (25°C) in 50 mM Tris (pH 8), 150 mM NaCl, 20 mM $MgCl_2$, 10% glycerol, 1 mM DTT, and 5 mM ATP. The reaction was started by the addition of 0.5 μM recombinant PafA-His_6 (a gift from Huilin Li) and stopped by the addition of 4 × SDS sample buffer and boiled for 5 min.

Phosphoribohydrolase Assay

The assay was adapted from a previously described method (Kurakawa et al., 2007). See Supplemental Experimental Procedures for details.

Sequence and Phylogenetic Analysis of Mycobacterial Log Homologs

Homologs of Log were obtained by performing iterative profile searches using the PSI-BLAST (Altschul et al., 1997) and JACKHMMER (Finn et al., 2011) programs, run against the non-redundant (NR) protein database of the NCBI, with various LOG domain-containing proteins as queries. See Supplemental Experimental Procedures for details.

M. tuberculosis Supernatant and Intracellular Cytokinin Measurements

For supernatant analysis, cultures were grown in triplicate in 7H9 medium to an OD_{580} of 1. Supernatant (36 ml) for each replicate was filter sterilized through

0.45 μm syringe filters and lyophilized (using a Labconco freeze-dry system). For cell lysates, cultures were grown in triplicate in Sauton's minimal media (Festa et al., 2010) up to an OD_{580} of 1. Cultures (35 ml) were pelleted and washed once in PBS. Each pellet was resuspended in 2 ml 70% ethanol + 0.004% of sodium diethyldithiocarbamic acid (DCC). Cells were lysed by bead beating with zirconia beads three times for 30 s. Supernatants were gently mixed with 2.5 ml 70% ethanol + 0.004% DCC for 24 hr at 4°C, before lyophilization. Measurement of cytokinins was performed as described previously (Novak et al., 2003; Svačinová et al., 2012; Tarkowski et al., 2010). See Supplemental Experimental Procedures for details.

Metabolomic Analysis of *M. tuberculosis* Cell Lysates

Cultures were grown in quadruplicate up to an OD_{580} of 1. Sixty-five OD equivalents per replicate were processed by chloroform:methanol extraction (Layre et al., 2011). Metabolomic profiling was carried out at Metabolon as previously described (Dehaven et al., 2010; Evans et al., 2009, 2012).

Cytokinin Oxidase Activity Assay

The assay was adapted from a method described previously (Frébort et al., 2002). See Supplemental Experimental Procedures for details.

SUPPLEMENTAL INFORMATION

Supplemental Information includes Supplemental Experimental Procedures, six figures, and four tables and can be found with this article online at http://dx.doi.org/10.1016/j.molcel.2015.01.024.

AUTHOR CONTRIBUTIONS

M.I.S. performed the suppressor screen; isolated, cloned, and biochemically characterized Rv1205; and performed all in vitro and in vivo *M. tuberculosis* work. S.T. performed all HPLC analysis. L.A. and L.M.I. carried out the genomic and evolutionary analysis. F.E.M. and S.P.G. did the liquid chromatography-tandem mass spectrometry (LC-MS/MS) analysis of Pup~Log. S.R.H. modeled the *M. tuberculosis* Log active site. O.N. and M.S. quantified the cytokinins. M.I.S. and K.H.D. wrote the manuscript.

ACKNOWLEDGMENTS

We are grateful to A. Darwin and C. Nathan for review of draft versions of this manuscript and to V. DiRita, I. Mohr, T. Richardson, and V. Torres for helpful suggestions. We thank D. Reinberg for generous support, W. Houry for *E. coli* LDC and advice, H. Li for purified PafA, S. Ehrt for the Δ*prcBA*::*hyg* mutant, B. Bennett and S. Butler-Wu for cloning assistance, J. McKinney for pMV306.Strep, H. Martínková and B. Pařízková for technical assistance in cytokinin detection, K. Rhee for metabolomics advice, R. Michalek at Metabolon for outstanding data analysis, and the Rockefeller Proteomics Resource Center for use of their facilities. We are eternally grateful to Charlie Rice and The Rockefeller University for providing laboratory space and support for the 15 months after Superstorm Sandy. This work was supported by NIH grant R01HL092774 (awarded to K.H.D.) and the Jan T. Vilcek Endowed Fellowship fund (awarded to M.I.S.). L.A. and L.M.I. are funded by the Intramural Research Program of the National Library of Medicine (NIH). For O.N. and M.S., work is supported by the Ministry of Education, Youth and Sport of the Czech Republic (grant LO1204 from the National Program of Sustainability I) and the Internal Grant Agency of Palacký University (IGA_PrF_2015_021). K.H.D holds an Investigators in the Pathogenesis of Infectious Disease Award from the Burroughs Wellcome Fund.

Received: October 16, 2014
Revised: December 17, 2014
Accepted: January 16, 2015
Published: February 26, 2015

REFERENCES

Altschul, S.F., Madden, T.L., Schäffer, A.A., Zhang, J., Zhang, Z., Miller, W., and Lipman, D.J. (1997). Gapped BLAST and PSI-BLAST: a new generation of protein database search programs. Nucleic Acids Res. *25*, 3389–3402.

Argueso, C.T., Ferreira, F.J., and Kieber, J.J. (2009). Environmental perception avenues: the interaction of cytokinin and environmental response pathways. Plant Cell Environ. *32*, 1147–1160.

Arnold, K., Bordoli, L., Kopp, J., and Schwede, T. (2006). The SWISS-MODEL workspace: a web-based environment for protein structure homology modelling. Bioinformatics *22*, 195–201.

Bjork, G.R. (1996). Stable RNA modification. In *Escherichia Coli* and *Salmonella*: Cellular and Molecular Biology, Second Edition, *Volume 1*, F.C. Neidhardt, ed. (Washington, DC: ASM Press), pp. 861–886.

Bowman, L.A., McLean, S., Poole, R.K., and Fukuto, J.M. (2011). The diversity of microbial responses to nitric oxide and agents of nitrosative stress close cousins but not identical twins. Adv. Microb. Physiol. *59*, 135–219.

Burns, K.E., Cerda-Maira, F.A., Wang, T., Li, H., Bishai, W.R., and Darwin, K.H. (2010). "Depupylation" of prokaryotic ubiquitin-like protein from mycobacterial proteasome substrates. Mol. Cell *39*, 821–827.

Cerda-Maira, F.A., Pearce, M.J., Fuortes, M., Bishai, W.R., Hubbard, S.R., and Darwin, K.H. (2010). Molecular analysis of the prokaryotic ubiquitin-like protein (Pup) conjugation pathway in *Mycobacterium tuberculosis*. Mol. Microbiol. *77*, 1123–1135.

Chan, J., Xing, Y., Magliozzo, R.S., and Bloom, B.R. (1992). Killing of virulent *Mycobacterium tuberculosis* by reactive nitrogen intermediates produced by activated murine macrophages. J. Exp. Med. *175*, 1111–1122.

Chan, J., Tanaka, K., Carroll, D., Flynn, J., and Bloom, B.R. (1995). Effects of nitric oxide synthase inhibitors on murine infection with *Mycobacterium tuberculosis*. Infect. Immun. *63*, 736–740.

Choi, J., Choi, D., Lee, S., Ryu, C.M., and Hwang, I. (2011). Cytokinins and plant immunity: old foes or new friends? Trends Plant Sci. *16*, 388–394.

Darwin, K.H., Ehrt, S., Gutierrez-Ramos, J.C., Weich, N., and Nathan, C.F. (2003). The proteasome of *Mycobacterium tuberculosis* is required for resistance to nitric oxide. Science *302*, 1963–1966.

Dehaven, C.D., Evans, A.M., Dai, H., and Lawton, K.A. (2010). Organization of GC/MS and LC/MS metabolomics data into chemical libraries. J. Cheminform. *2*, 9.

Delley, C.L., Striebel, F., Heydenreich, F.M., Özcelik, D., and Weber-Ban, E. (2012). Activity of the mycobacterial proteasomal ATPase Mpa is reversibly regulated by pupylation. J. Biol. Chem. *287*, 7907–7914.

Evans, A.M., DeHaven, C.D., Barrett, T., Mitchell, M., and Milgram, E. (2009). Integrated, nontargeted ultrahigh performance liquid chromatography/electrospray ionization tandem mass spectrometry platform for the identification and relative quantification of the small-molecule complement of biological systems. Anal. Chem. *81*, 6656–6667.

Evans, A.M., Mitchell, M., Dai, H., and DeHaven, C.D. (2012). Categorizing ion-features in liquid chromatography/mass spectrometry metobolomics data. Metabolomics *2*, 110.

Festa, R.A., Pearce, M.J., and Darwin, K.H. (2007). Characterization of the proteasome accessory factor (paf) operon in Mycobacterium tuberculosis. J. Bacteriol. *189*, 3044–3050.

Festa, R.A., McAllister, F., Pearce, M.J., Mintseris, J., Burns, K.E., Gygi, S.P., and Darwin, K.H. (2010). Prokaryotic ubiquitin-like protein (Pup) proteome of *Mycobacterium tuberculosis* [corrected]. PLoS ONE *5*, e8589.

Festa, R.A., Jones, M.B., Butler-Wu, S., Sinsimer, D., Gerads, R., Bishai, W.R., Peterson, S.N., and Darwin, K.H. (2011). A novel copper-responsive regulon in *Mycobacterium tuberculosis*. Mol. Microbiol. *79*, 133–148.

Finn, R.D., Clements, J., and Eddy, S.R. (2011). HMMER web server: interactive sequence similarity searching. Nucleic Acids Res. *39*, W29–W37.

Frébort, I., Sebela, M., Galuszka, P., Werner, T., Schmülling, T., and Pec, P. (2002). Cytokinin oxidase/cytokinin dehydrogenase assay: optimized procedures and applications. Anal. Biochem. *306*, 1–7.

Frébort, I., Kowalska, M., Hluska, T., Frébortová, J., and Galuszka, P. (2011). Evolution of cytokinin biosynthesis and degradation. J. Exp. Bot. *62*, 2431–2452.

Gandotra, S., Schnappinger, D., Monteleone, M., Hillen, W., and Ehrt, S. (2007). *In vivo* gene silencing identifies the *Mycobacterium tuberculosis* proteasome as essential for the bacteria to persist in mice. Nat. Med. *13*, 1515–1520.

Gandotra, S., Lebron, M.B., and Ehrt, S. (2010). The *Mycobacterium tuberculosis* proteasome active site threonine is essential for persistence yet dispensable for replication and resistance to nitric oxide. PLoS Pathog. *6*, e1001040.

Garbe, T.R., Barathi, J., Barnini, S., Zhang, Y., Abou-Zeid, C., Tang, D., Mukherjee, R., and Young, D.B. (1994). Transformation of mycobacterial species using hygromycin resistance as selectable marker. Microbiology *140*, 133–138.

Imkamp, F., Striebel, F., Sutter, M., Ozcelik, D., Zimmermann, N., Sander, P., and Weber-Ban, E. (2010). Dop functions as a depupylase in the prokaryotic ubiquitin-like modification pathway. EMBO Rep. *11*, 791–797.

Kamada-Nobusada, T., and Sakakibara, H. (2009). Molecular basis for cytokinin biosynthesis. Phytochemistry *70*, 444–449.

Komander, D., and Rape, M. (2012). The ubiquitin code. Annu. Rev. Biochem. *81*, 203–229.

Kurakawa, T., Ueda, N., Maekawa, M., Kobayashi, K., Kojima, M., Nagato, Y., Sakakibara, H., and Kyozuka, J. (2007). Direct control of shoot meristem activity by a cytokinin-activating enzyme. Nature *445*, 652–655.

Lamichhane, G., Raghunand, T.R., Morrison, N.E., Woolwine, S.C., Tyagi, S., Kandavelou, K., and Bishai, W.R. (2006). Deletion of a *Mycobacterium tuberculosis* proteasomal ATPase homologue gene produces a slow-growing strain that persists in host tissues. J. Infect. Dis. *194*, 1233–1240.

Layre, E., Sweet, L., Hong, S., Madigan, C.A., Desjardins, D., Young, D.C., Cheng, T.Y., Annand, J.W., Kim, K., Shamputa, I.C., et al. (2011). A comparative lipidomics platform for chemotaxonomic analysis of *Mycobacterium tuberculosis*. Chem. Biol. *18*, 1537–1549.

Layre, E., Lee, H.J., Young, D.C., Martinot, A.J., Buter, J., Minnaard, A.J., Annand, J.W., Fortune, S.M., Snider, B.B., Matsunaga, I., et al. (2014). Molecular profiling of *Mycobacterium tuberculosis* identifies tuberculosinyl nucleoside products of the virulence-associated enzyme Rv3378c. Proc. Natl. Acad. Sci. USA *111*, 2978–2983.

Lin, G., Li, D., de Carvalho, L.P., Deng, H., Tao, H., Vogt, G., Wu, K., Schneider, J., Chidawanyika, T., Warren, J.D., et al. (2009). Inhibitors selective for mycobacterial versus human proteasomes. Nature *461*, 621–626.

MacMicking, J.D., North, R.J., LaCourse, R., Mudgett, J.S., Shah, S.K., and Nathan, C.F. (1997). Identification of nitric oxide synthase as a protective locus against tuberculosis. Proc. Natl. Acad. Sci. USA *94*, 5243–5248.

McLennan, A.G. (2006). The Nudix hydrolase superfamily. Cell. Mol. Life Sci. *63*, 123–143.

Novak, O., Tarkowski, P., Tarkowski, D., Dolezal, K., Lenobel, R., and Strnad, M. (2003). Quantitative analysis of cytokinins in plants by liquid chromatography–single-quadrupole mass spectrometry. Anal. Chim. Acta *480*, 207–218.

Pearce, M.J., Mintseris, J., Ferreyra, J., Gygi, S.P., and Darwin, K.H. (2008). Ubiquitin-like protein involved in the proteasome pathway of *Mycobacterium tuberculosis*. Science *322*, 1104–1107.

Pertry, I., Václavíková, K., Depuydt, S., Galuszka, P., Spíchal, L., Temmerman, W., Stes, E., Schmülling, T., Kakimoto, T., Van Montagu, M.C., et al. (2009). Identification of *Rhodococcus fascians* cytokinins and their modus operandi to reshape the plant. Proc. Natl. Acad. Sci. USA *106*, 929–934.

Popelková, H., Fraaije, M.W., Novák, O., Frébortová, J., Bilyeu, K.D., and Frébort, I. (2006). Kinetic and chemical analyses of the cytokinin dehydrogenase-catalysed reaction: correlations with the crystal structure. Biochem. J. *398*, 113–124.

Poulsen, C., Akhter, Y., Jeon, A.H., Schmitt-Ulms, G., Meyer, H.E., Stefanski, A., Stühler, K., Wilmanns, M., and Song, Y.H. (2010). Proteome-wide identification of mycobacterial pupylation targets. Mol. Syst. Biol. *6*, 386.

Ramakrishnan, L., Federspiel, N.A., and Falkow, S. (2000). Granuloma-specific expression of *Mycobacterium* virulence proteins from the glycine-rich PE-PGRS family. Science *288*, 1436–1439.

Sakakibara, H. (2006). Cytokinins: activity, biosynthesis, and translocation. Annu. Rev. Plant Biol. *57*, 431–449.

Sassetti, C.M., Boyd, D.H., and Rubin, E.J. (2001). Comprehensive identification of conditionally essential genes in mycobacteria. Proc. Natl. Acad. Sci. USA *98*, 12712–12717.

Sassetti, C.M., Boyd, D.H., and Rubin, E.J. (2003). Genes required for mycobacterial growth defined by high density mutagenesis. Mol. Microbiol. *48*, 77–84.

Schauenstein, E., Esterbauer, H., and Zollner, H. (1977). Aldehydes in Biological Systems: Their Natural Occurrence and Biological Activities. (London: Pion).

Schmidt, M., and Finley, D. (2014). Regulation of proteasome activity in health and disease. Biochim. Biophys. Acta *1843*, 13–25.

Shi, X., Festa, R.A., Ioerger, T.R., Butler-Wu, S., Sacchettini, J.C., Darwin, K.H., and Samanovic, M.I. (2014). The copper-responsive RicR regulon contributes to Mycobacterium tuberculosis virulence. mBio *5*, e00876-13.

Shiloh, M.U., and Nathan, C.F. (2000). Reactive nitrogen intermediates and the pathogenesis of *Salmonella* and mycobacteria. Curr. Opin. Microbiol. *3*, 35–42.

Söding, J., Biegert, A., and Lupas, A.N. (2005). The HHpred interactive server for protein homology detection and structure prediction. Nucleic Acids Res. *33*, W244–W248.

Striebel, F., Imkamp, F., Sutter, M., Steiner, M., Mamedov, A., and Weber-Ban, E. (2009). Bacterial ubiquitin-like modifier Pup is deamidated and conjugated to substrates by distinct but homologous enzymes. Nat. Struct. Mol. Biol. *16*, 647–651.

Svačinová, J., Novák, O., Plačková, L., Lenobel, R., Holík, J., Strnad, M., and Doležal, K. (2012). A new approach for cytokinin isolation from Arabidopsis tissues using miniaturized purification: pipette tip solid-phase extraction. Plant Methods *8*, 17.

Tarkowski, P., Václavíková, K., Novák, O., Pertry, I., Hanuš, J., Whenham, R., Vereecke, D., Šebela, M., and Strnad, M. (2010). Analysis of 2-methylthio-derivatives of isoprenoid cytokinins by liquid chromatography-tandem mass spectrometry. Anal. Chim. Acta *680*, 86–91.

Tomko, R.J., Jr., and Hochstrasser, M. (2013). Molecular architecture and assembly of the eukaryotic proteasome. Annu. Rev. Biochem. *82*, 415–445.

Urbonavicius, J., Qian, Q., Durand, J.M., Hagervall, T.G., and Björk, G.R. (2001). Improvement of reading frame maintenance is a common function for several tRNA modifications. EMBO J. *20*, 4863–4873.

Wang, T., Darwin, K.H., and Li, H. (2010). Binding-induced folding of prokaryotic ubiquitin-like protein on the *Mycobacterium* proteasomal ATPase targets substrates for degradation. Nat. Struct. Mol. Biol. *17*, 1352–1357.

Watrous, J., Burns, K., Liu, W.T., Patel, A., Hook, V., Bafna, V., Barry, C.E., 3rd, Bark, S., and Dorrestein, P.C. (2010). Expansion of the mycobacterial "PUPylome". Mol. Biosyst. *6*, 376–385.

Molecular Cell

Supplemental Information

Proteasomal Control of Cytokinin Synthesis Protects *Mycobacterium tuberculosis* against Nitric Oxide

Marie I. Samanovic, Shengjiang Tu, Ondřej Novák, Lakshminarayan M. Iyer, Fiona E. McAllister, L. Aravind, Steven P. Gygi, Stevan R. Hubbard, Miroslav Strnad, and K. Heran Darwin

Samanovic *et al*
Figure S1

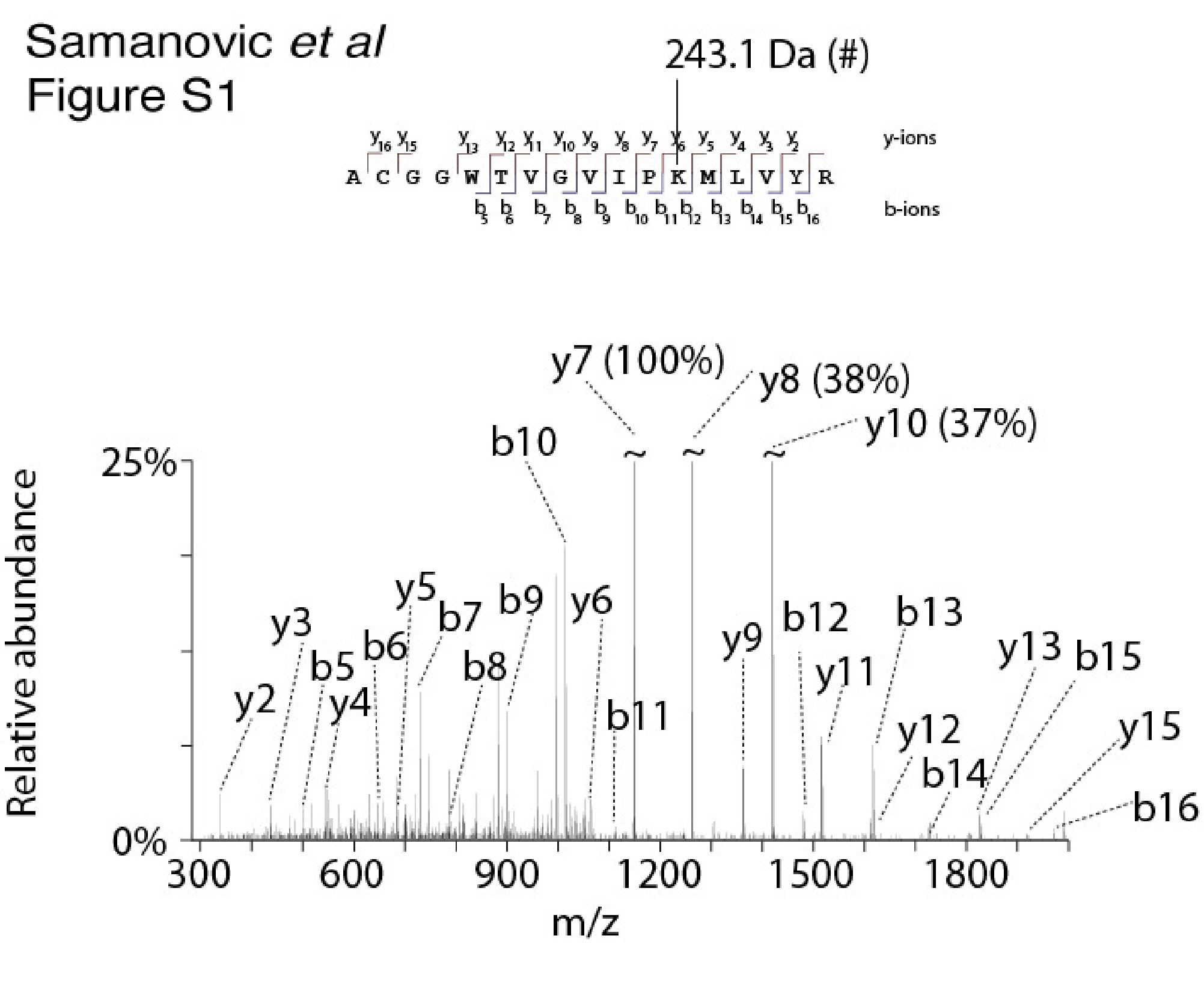

Samanovic *et al*
Figure S2

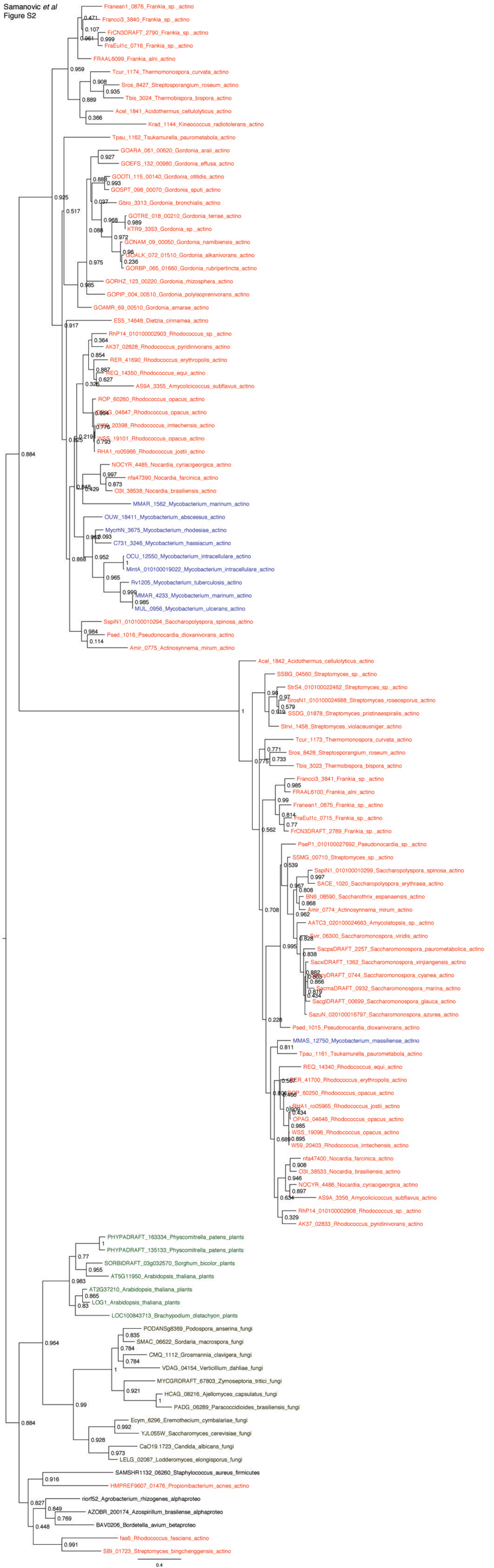

Samanovic *et al*
Figure S3

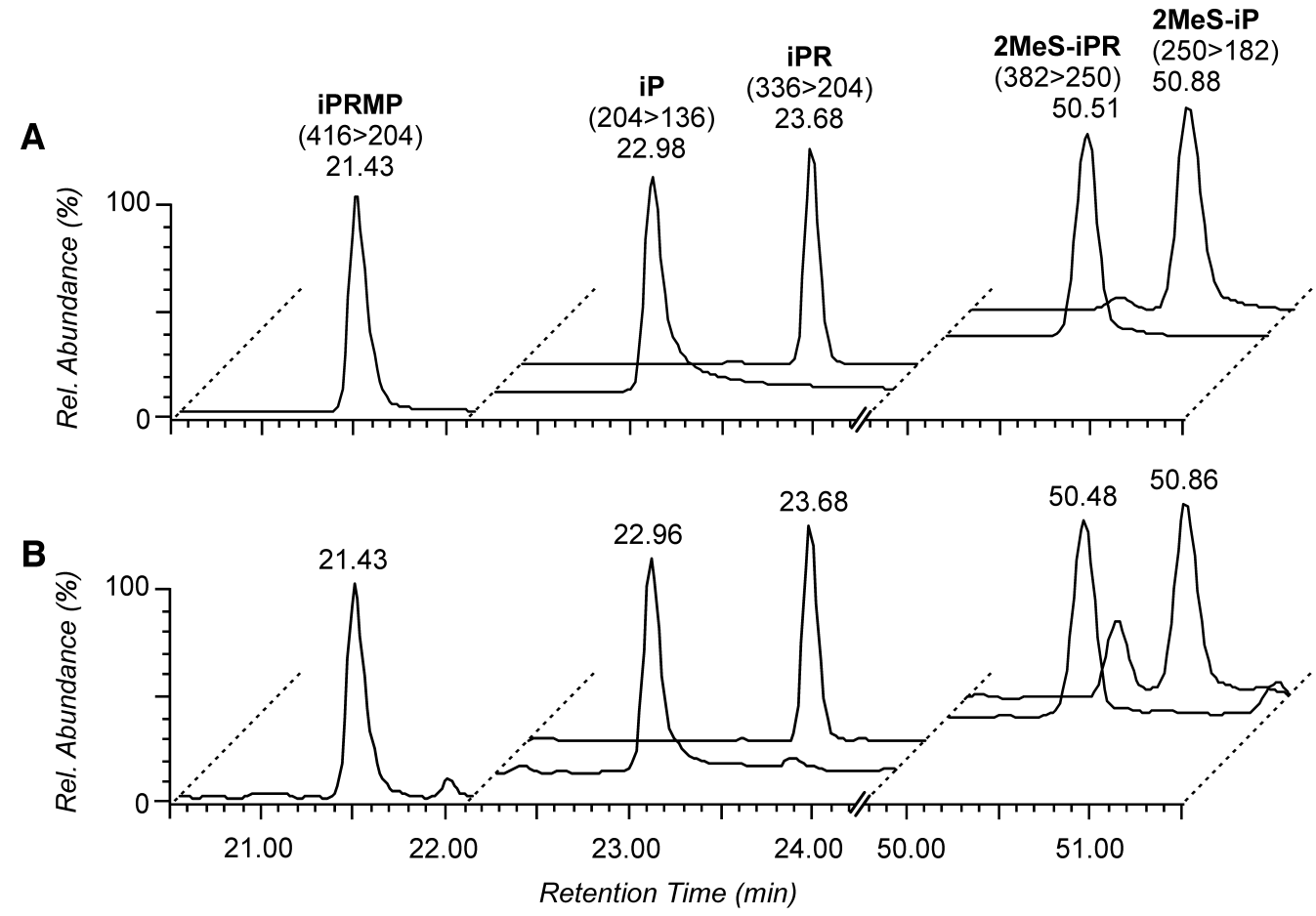

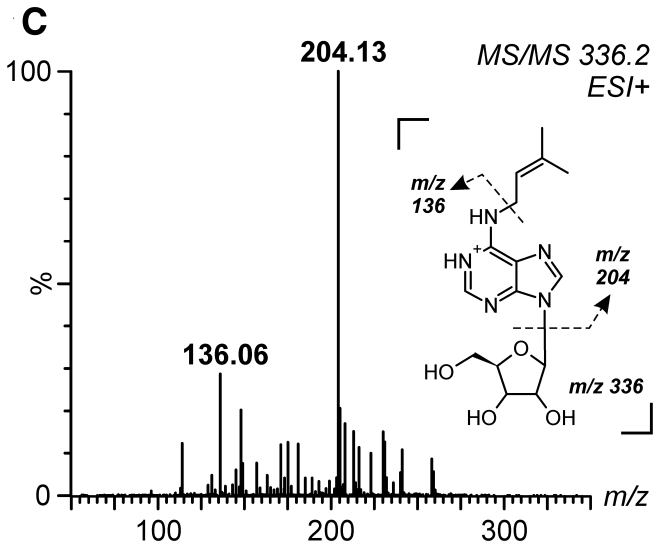

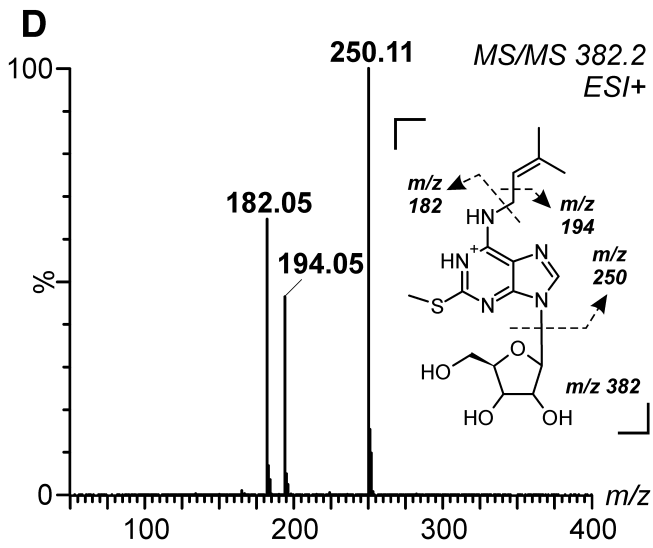

Samanovic *et al*
Figure S4

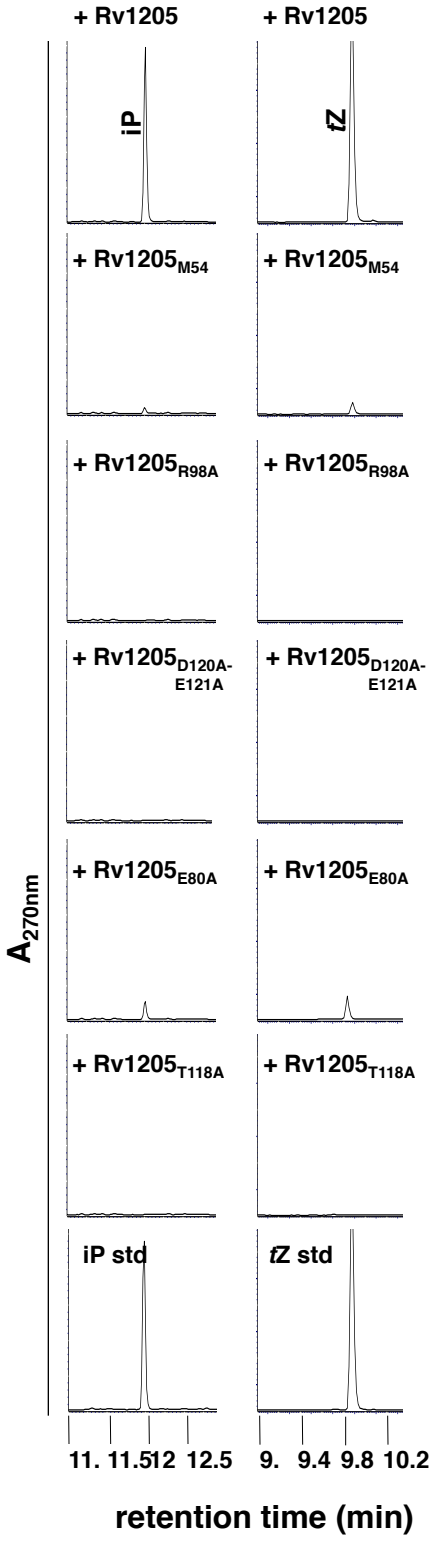

Samanovic *et al*
Figure S5

A

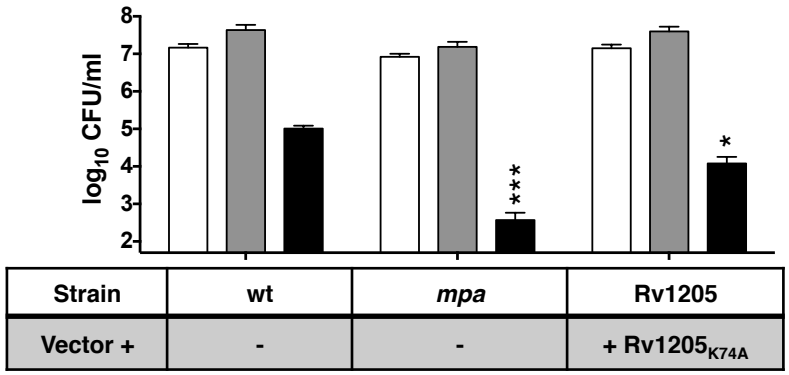

B

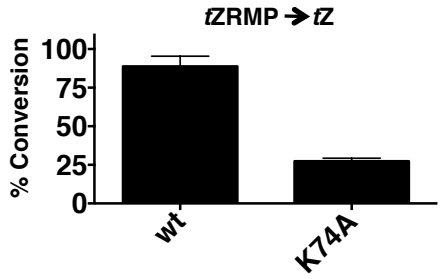

Samanovic *et al*
Figure S6

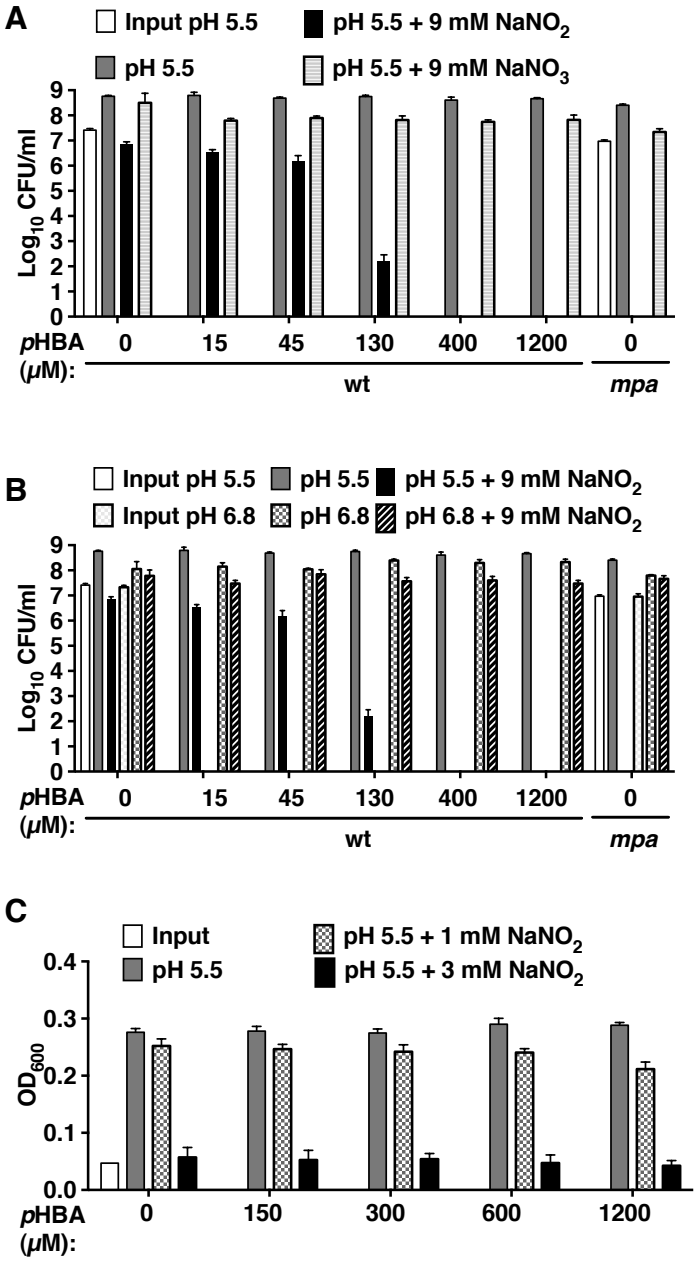

Supplemental figure legends

Figure S1. Evidence for isopeptide linkage between Rv1205 lysine 74 and the C-terminus of Pup. Related to Figure 2D. See Extended Experimental Procedures for details.

Figure S2. Expanded version of the phylogenetic analysis of Log homologues. Related to Figure 3C. Proteins are represented by their gene names, species names and their taxonomic lineage separated by underscores. Bootstrap values are indicated at each node.

Figure S3: Natural occurrence of isopentenyladenine (iP)-type cytokinins in an *M. tuberculosis mpa* mutant. Related to Table 1. (A) Multi-reaction monitoring (MRM) chromatograms of iP-type cytokinin standards injected onto a reversed-phase chromatographic column (isopentenyladenine, iP 204>136; isopentenyladenosine, iPR 336>204; isopentenyladenosine monophosphate, iPRMP 416>204; 2-methylthio-isopentenyladenine, 2MeS-iP 250>182; 2-methylthio-isopentenyladenosine, 2MeS-iPR 382>250). (B) Identification of endogenous iP-type cytokinins in cell lysate extracts on coincident retention times and selected ion monitoring bases. (C) and (D) MS/MS confirmation spectra of endogenous iPR (C) and 2MeS-iPR (D) validate the presence of iP-type cytokinins in *M. tuberculosis*.

Figure S4: Conversion rate of iPRMP and *t*ZRMP to iP and *t*Z by Rv1205 mutants. Related to Figure 4F. iPRMP and *t*ZRMP were used as substrates, after 20 min. "std" = standards**.**

Figure S5: $Rv1205_{K74A}$ accumulation sensitizes *M. tuberculosis* to NO. Related to Figure 5. (A) NO susceptibility assay of wt bacteria, *mpa*, and wt expressing $Rv1205_{K74A}$. All strains

harbor an integrated pMV306.strep vector with or without the indicated gene. (-) indicates empty vector. CFU of surviving bacteria after exposure to acidified media without (grey bars) or with (black bars) nitrite. Open bars show input CFU. Data show means ± standard deviation (SD), n = 6, from two independent combined experiments. All samples exposed to $NaNO_2$ were compared to wt with two-tailed Student's *t*-test; * $p < 0.05$; *** $p < 0.001$. (B) Phosphoribohydrolase activity towards *t*ZRMP as measured by HPLC using $Rv1205_{K74A}$ (means ± SD, n = 3). *t*ZRMP: *trans*-zeatin-riboside monophosphate; *t*Z: *trans*-zeatin.

Figure S6. Increasing concentrations of *p*HBA sensitized wt *M. smegmatis* (A) and (B) but not *E. coli* (C) to NO. Related to Figure 6. (A) and (B) *M. smegmatis* nitrite sensitivity was assessed with exposure to 9 mM concentration of $NaNO_2$ under acidic condition. CFU of surviving bacteria after exposure to acidified media without (grey bars, pH 5.5) or with nitrite (black bars, pH 5.5 + 9 mM $NaNO_2$). Open bars show input CFU. Stripped bars show acidified nitrate control (pH 5.5 + 9 mM $NaNO_3$, (A)), and neutral pH control (pH 6.8 +/- $NaNO_2$, (B)). (C) *E. coli* nitrite sensitivity was tested by exposing cultures to MES-buffered LB (pH 5) +/- sodium nitrite (1 and 3 mM) in 96-well plates. OD_{600} were measured after 24 hours to measure for growth. OD_{600} of cultures in acidified media without (grey bars) or with nitrite (black and striped bars). Open bars show starting OD_{600}. Data show means ± SD, n = 3.

Table S1: Bacterial strains, plasmids and primers used in this work. See Excel file.

Table S2: Cytokinin levels in *M. tuberculosis* cell media and lysates. Related to Table 1. Cytokinin levels and nucleotide precursors in supernatants of *M. tuberculosis* cultures at OD_{580} = 1 ("MEDIA") (wt, *mpa*, *sup1* and *sup1* with $Rv1205_{D120A,E121A}$ respectively strain MHD1, 149, 718, 777) and in 1 g of pelleted of *M. tuberculosis* cells ("LYSATES") (wt, *mpa*, Rv1205, *sup1* and *sup1* with $Rv1205_{D120A,E121A}$ respectively strains MHD1, 149, 718, 726, 777). Values are in pmol/l; mean ± SD, n=3. Statistically significant values are indicated in bold. Asterisks indicate statistically significant difference in mutant lines versus wt with an ANOVA analysis (*, **, and *** correspond to p-values of $0.05 > p > 0.01$, $0.01 > p > 0.001$, and $p < 0.001$, respectively). LOD: limit of detection, defined as a signal to noise ratio of 3:1. iP: isopentenyladenine; *t*Z: *trans*-zeatin; *c*Z: *cis*-zeatin, DHZ: dihydrozeatin; R: riboside (adenosine); MP: monophosphate; G: glucoside; MeS: methylthio.

MEDIA	wt			*mpa*				*sup1*				*sup1* + Rv1205$_{D120A,E121A}$			
***t*Z**	0.16	±	0.04	0.15	±	0.04		**0.015**	**±**	**0.003**	**	**0.029**	**±**	**0.004**	**
***t*ZR**		<LOD			<LOD				<LOD			0.157	±	0.004	
***t*ZRMP**		<LOD			<LOD				<LOD			0.359	±	0.036	
***t*ZOG**		<LOD			<LOD				<LOD				<LOD		
***t*ZROG**		<LOD			<LOD				<LOD				<LOD		
***t*Z7G**	1.36	±	0.30	1.68	±	0.36		1.76	±	0.450			<LOD		
***t*Z9G**		<LOD			<LOD				<LOD				<LOD		
2MeS-*t*Z		<LOD			<LOD				<LOD				<LOD		
2MeS-*t*ZR	86.19	±	6.08	**40.18**	**±**	**4.71**	**	**132.86**	**±**	**17.364**	*	**54.042**	**±**	**15.142**	*
***c*Z**	0.16	±	0.02	0.15	±	0.033		0.11	±	0.027		0.066	±	0.007	**
***c*ZR**	0.03	±	0.01	0.03	±	0.008		0.03	±	0.005			<LOD		
***c*ZRMP**		<LOD			<LOD				<LOD				<LOD		
***c*ZOG**		<LOD			<LOD				<LOD				<LOD		
***c*ZROG**		<LOD			<LOD				<LOD				<LOD		
***c*Z9G**		<LOD			<LOD				<LOD				<LOD		
2MeS-*c*Z		<LOD			<LOD				<LOD				<LOD		
2MeS-*c*ZR	29.03	±	7.85	**12.67**	**±**	**1.801**	*	47.58	±	6.99		**11.318**	**±**	**3.036**	*
DHZ		<LOD			<LOD				<LOD				<LOD		
DHZR	0.05	±	0.01	**0.022**	**±**	**0.006**	*	0.139	±	0.035	*	0.376	±	0.021	***
DHZRMP		<LOD			<LOD				<LOD				<LOD		
DHZOG	0.83	±	0.21	1.14	±	0.30		0.37	±	0.09	*		<LOD		
DHZROG		<LOD			<LOD				<LOD				<LOD		
DHZ7G	1.04	±	0.24	1.22	±	0.16		0.86445	±	0.17			<LOD		
DHZ9G		<LOD			<LOD				<LOD				<LOD		
iP	234.39	±	18.03	258.44	±	36.17		**7.8**	**±**	**1.7**	***	**10.57**	**±**	**1.49**	***
iPR	47.52	±	5.65	**10.92**	**±**	**1.00**	***	**121.10**	**±**	**20.06**	**	**260.18**	**±**	**24.66**	***
iPRMP	11.15	±	1.17	9.29	±	0.27		10.05	±	0.31		**6.59**	**±**	**0.46**	**
iP7G		<LOD			<LOD				<LOD				<LOD		
iP9G		<LOD			<LOD				<LOD				<LOD		
2MeS-iP	6184.9	±	191.77	**10293.6**	**±**	**1441.7**	*	**61.4**	**±**	**15.8**	***	**17.51**	**±**	**0.55**	***
2MeS-iPR	5830.9	±	141.05	**3013.1**	**±**	**523.0**	**	**10243.2**	**±**	**1671.2**	*	**12354.6**	**±**	**1616.2**	**

LYSATE	wt			*mpa*			*sup1*				Rv1205				*sup1* + Rv1205$_{D120A,E121A}$			
***t*Z**	1.33	±	0.24	1.23	±	0.19	**0.65**	**±**	**0.17**	*	**3.60**	**±**	**0.91**	*	**2.48**	**±**	**0.24**	**
***t*ZR**	0.71	±	0.16	0.95	±	0.19	0.92	±	0.10		**1.56**	**±**	**0.31**	*	0.79	±	0.05	
***t*ZRMP**		<LOD			<LOD			<LOD				<LOD				<LOD		
***t*ZOG**		<LOD			<LOD			<LOD				<LOD				<LOD		
***t*ZROG**		<LOD			<LOD			<LOD				<LOD				<LOD		
***t*Z7G**		<LOD			<LOD			<LOD				<LOD				<LOD		
***t*Z9G**		<LOD			<LOD			<LOD				<LOD				<LOD		
2MeS-*t*Z		<LOD			<LOD			<LOD				<LOD				<LOD		
2MeS-*t*ZR	49.28	±	10.46	89.20	±	30.49	58.69	±	15.89		33.72	±	11.48		55.01	±	4.27	
***c*Z**	1.98	±	0.15	1.92	±	0.32	2.21	±	0.28		**3.26**	**±**	**0.24**	**	**2.76**	**±**	**0.08**	**
***c*ZR**	2.41	±	0.43	**1.49**	**±**	**0.18**	*	3.26	±	0.21	3.30	±	0.56		**6.02**	**±**	**0.17**	***
***c*ZRMP**		<LOD			<LOD			<LOD				<LOD				<LOD		
***c*ZOG**		<LOD			<LOD			<LOD				<LOD				<LOD		
cZROG		<LOD			<LOD			<LOD				<LOD				<LOD		
***c*Z9G**		<LOD			<LOD			<LOD				<LOD				<LOD		
2MeS-*c*Z		<LOD			<LOD			<LOD				<LOD				<LOD		
2MeS-*c*ZR		<LOD			<LOD			<LOD				<LOD				<LOD		
DHZ		<LOD			<LOD			<LOD				<LOD				<LOD		
DHZR	1.73	±	0.10	1.48	±	0.31	2.20	±	0.38		3.68	±	0.78	*	1.15	±	0.35	
DHZRMP		<LOD			<LOD			<LOD				<LOD				<LOD		
DHZOG		<LOD			<LOD			<LOD				<LOD				<LOD		
DHZROG		<LOD			<LOD			<LOD				<LOD				<LOD		
DHZ7G		<LOD			<LOD			<LOD				<LOD				<LOD		
DHZ9G		<LOD			<LOD			<LOD				<LOD				<LOD		
iP	121.09	±	21.88	89.66	±	6.75	**30.17**	**±**	**4.01**	**	**27.11**	**±**	**3.33**	**	**21.7**	**±**	**1.2**	**
iPR	125.81	±	7.55	**39.12**	**±**	**8.23**	***	**822.9**	**±**	**177.9**	**	**983.6**	**±**	**169.3**	**	**352.5**	**±**	**76.72**	*
iPRMP	298.74	±	49.81	**185.72**	**±**	**18.68**	*	**3596**	**±**	**640**	**	**2021.8**	**±**	**319.1**	**	**1750**	**±**	**379.3**	**
iP7G		<LOD			<LOD			<LOD				<LOD				<LOD		
iP9G		<LOD			<LOD			<LOD				<LOD				<LOD		
2MeS-iP	11917	±	1620	12131	±	1091.8	**183.7**	**±**	**59.1**	***	**141.5**	**±**	**38.6**	***	**222.8**	**±**	**75.0**	***
2MeS-iPR	19896	±	2441	**8164.8**	**±**	**195.8**	**	29614	±	5139	**40724**	**±**	**6622**	*	**29187**	**±**	**2729**	*

Significantly altered metabolites	***mpa*** **wt**	***sup1*** **wt**	***log*** **wt**	***sup1*** ***mpa***	***log*** ***mpa***	***log*** ***sup1***
Total metabolites $p \leq 0.05$	32	20	22	76	113	84
metabolites (↑|↓)	27|5	12|8	6|16	18|58	35|78	35|49
Total metabolites $0.05 < p < 0.10$	18	11	19	22	26	24
metabolites (↑|↓)	8|10	2|9	2|17	5|17	7|19	9|15

Table S3: Statistical summary of significantly altered metabolites comparing wt, *mpa*, *sup1* and *log* strains intracellular contents. Related to Figure 6A. A total of 220 metabolites were detected and Welch's two-sample *t*-test was used to identify those that differed significantly between experimental groups. The number of metabolites that achieved statistical significance ($p \leq 0.05$), as well as those approaching significance ($0.05 < p < 0.10$) in showing a fold of change between two groups ≥1 are indicated in red, and <1 in green. For example, in the "*mpa*/wt" sample, 27 metabolites were statistically significantly increased in the *mpa* mutant compared to in the wt, while five were reduced.

Table S4: Heat map comparing metabolite levels in wt, *mpa*, *sup1* and *log* strains (MHD1, 149, 718 and 726). Related to Figure 6A. This table includes raw data, results of statistical tests, *p*-values, and *q*-values. See Excel file.

Supplemental Information

Extended Experimental Procedures

Bacterial strains, plasmids and culture conditions

M. tuberculosis strains were grown in Middlebrook 7H9 broth (Difco) supplemented with 0.2% glycerol, 0.05% Tween-80, 0.5% fraction V bovine serum albumin, 0.2% dextrose and 0.085% sodium chloride ("7H9"). *M. tuberculosis* cultures were grown without shaking in 25 or 75 cm^2 vented flasks (Corning) at 37ºC. 7H11 agar (Difco) supplemented with 0.5% glycerol and BBL ™ Middlebrook OADC enrichment (BD) was used for growth on solid medium ("7H11"). *M. tuberculosis* were transformed as described elsewhere (Hatfull and Jacobs, 2000).

E. coli strains used for cloning and expression were grown in LB-Miller broth (Difco) at 37°C with aeration on a shaker or on LB agar. *E. coli* strains were chemically transformed as previously described (Sambrook et al., 1989). The final concentrations of antibiotics used for *M. tuberculosis*: kanamycin, 50 μg/ml or kan^{50}; hygromycin, 50 μg/ml or hyg^{50}; streptomycin, 25 μg/ml or $strept^{25}$; and for *E. coli*: hygromycin, 150 μg/ml; kanamycin, 100 μg/ml; and streptomycin 50 μg/ml.

Site directed mutagenesis of plasmids was performed by sewing overlap extension (SOE) as described elsewhere (Horton, 1997). For isolation of mutations in specific genes we screened our ordered collection of 10,100 ΦMycoMarT7 mutants as described elsewhere (Festa et al., 2007). The D*mpa*::*hyg* mutant was made by deletion-disruption mutagenesis as described in detail elsewhere using pYUB854 (Festa et al., 2011).

Southern Blotting of chromosomal DNA

*M. tuberculosis g*enomic DNA was extracted (van Helden et al., 2001) and digested with BamHI, subjected to 0.8% agarose gel electrophoresis before capillary transfer to a nitrocellulose membrane (Protran, Whatman) according to standard protocols (Ausubel, 2002). To probe for the *neo* gene encoded in ΦMycoMarT7, pKD13 was digested with BglII and ClaI; 170 ng of fragment encoding *neo* was boiled for 5 min, cooled on ice immediately and incubated for 2 hours with 1 μl Klenow enzyme (New England Biolabs), 0.1 U of random hexamers (Promega), 350 μg/ml bovine serum albumin (New England Biolabs), 0.04 mCi ^{32}P-deoxyadenosine-5'-triphosphate (MP Biomedicals), 200 mM HEPES, pH 6, and 20 μM CGT nucleotide mix (Invitrogen). Hybridization and detection with α-^{32}P-labeled probe was performed using a standard protocol (Ausubel, 2002).

Mouse infections

7-9 week old female C57BL6/J mice (Jackson Laboratories) were infected by aerosol to deliver ~200 bacilli per mouse, using a Glas-Col Inhalation Exposure System (Terre Haute, IN). Strains used were wt (MHD761), *mpa* (MHD762), *sup1* (MHD757) and Rv1205 (MHD763). Mice were humanely sacrificed according to an approved Institutional Animal Care and Use Committee protocol. Lungs and spleens were harvested and homogenized PBS-tween (0.05%) at indicated time points in order to determine bacterial colony forming units (CFU). Data were analyzed for statistical significance by a two-way ANOVA followed by a Bonferroni post-test.

Protein purification and immunoblotting

Recombinant proteins were produced in *E. coli* ER2566 and purified under native conditions

according to the manufacturer's specifications (Qiagen). Proteins were quantified by Bradford's method (Bio-Rad). Polyclonal rabbit antibodies were raised by Covance (Denver, PA). For all immunoblots, cell lysates or purified proteins were separated by either 4-15% gradient TGX Bio-Rad precast gel for anti-GlpK blots; 15% sodium dodecyl sulfate polyacrylamide gel electrophoresis (SDS-PAGE) for immunoblots detecting recombinant Rv1205 or 12% SDS-PAGE for immunoblots detecting Rv1205 in *M. tuberculosis* cell lysates; transferred to nitrocellulose and incubated with rabbit polyclonal antibodies to Rv1205-His_6. Equal loading was determined by stripping the nitrocellulose membranes with 0.2 N NaOH for 5 min, rinsing, blocking and incubating the nitrocellulose with polyclonal rabbit antibodies to dihydrolipoamide acyltransferase (DlaT) (Darwin et al., 2005; Tian et al., 2005). Horseradish peroxidase-conjugated anti-rabbit or anti-mouse secondary antibodies (GE-Amersham Biosciences) were used for chemiluminescent detection (SuperSignal West Pico or Femto Chemiluminescent substrate; ThermoScientific).

Recombinant Rv1205 protein dimers purified from *E. coli* were separated under non-denaturing conditions by 4-15% gradient TGX gels (Bio-Rad). Monomeric Rv1205 was made by mixing recombinant protein with SDS-loading buffer and boiled for 10 min.

Sequence and phylogenetic analysis of mycobacterial Log homologues

A multiple sequence alignment of selected homologues was built by the Kalign2 program (Lassmann et al., 2009) followed by manual adjustments based on profile-profile and structural adjustments. Domain architectures for LOG homologues were obtained using the Pfam database (Finn et al., 2010). Phylogenetic analysis was conducted using an approximately maximum-likelihood method implemented in the FastTree 2.1 (Price et al., 2010) program under default

parameters. Gene neighborhoods were obtained using a custom PERL script of the in-house TASS package. The script uses either the PTT file (downloadable from the NCBI ftp site) or the Genbank file, in the case of whole genome shot-gun sequences to extract neighbors of a given query gene.

Phosphoribohydrolase assay

For conversion analysis, recombinant protein activity was measured by incubating 2.5 μM Log-His_6 in a reaction mixture (50 mM Tris, 1 mM $MgCl_2$, 1 mM dithiothreitol, pH 7) with 10 μM substrate, at 30˚C. We observed that maximum hydrolysis was reached after 20 min therefore for all presented experiments we stopped reactions with three volumes of acetone at 20 min, and stored at -80˚C for 30 min. Insoluble material was removed by centrifugation at 15,000 *g* for 15 min, at 4˚C and the supernatant was dried by evaporation (55˚C on a hot plate). The resulting material was dissolved in 2% acetic acid, separated and quantified by Thermo Finnigan Surveyor Plus HPLC with a reverse phase C18 column (Symmetry, 4.6 mm × 150 mm, 3.5 μm particle size, Waters). Mobile phase included buffer A (5% acetonitrile, 0.1% TFA) and buffer B (90% acetonitrile, 0.1% TFA). The column was equilibrated using 100% buffer A from 0-5 min. A linear gradient from 0% B to 100% B was applied from 5-20 min for HPLC separation. Cytokinins were monitored and quantified by UV absorbance at 270 nm. For determination of kinetic parameters of Log for iPRMP and AMP substrates, 1 μM Log-His_6 was used with various concentration of substrates. GraphPad Prism was used to calculate the kinetics.

Liquid chromatography-mass spectrometry (LC-MS/MS) of Pup~Log

85 μl of an *in vitro* Log-pupylation reaction was separated by SDS-PAGE and stained with Coomassie brilliant blue (Bio-Safe Coomassie, Bio-Rad). Pup~Log was excised from the gel, cut

into 1 mm cubes and digested with trypsin overnight at 37 ºC. The resulting peptides were then purified using Stage Tips (Rappsilber et al., 2003), dried by vacuum centrifugation and then resuspended in 8 μl 5% formic acid of which 4 μl was analyzed on an LTQ Orbitrap Velos (Thermo Fisher Scientific, San Jose, CA) mass spectrometer. LC-MS/MS analysis was similar to as described previously using an LTQ Orbitrap Velos coupled to an Agilent 1200 series binary pump and a Famos autosampler (LC Packings, San Francisco, CA) (Burns et al., 2012). A hand-pulled fused silica microcapillary column (125 μm × 20 cm) was used for peptide separation and flow rates over the column of 300 nl/min were achieved using a flow-split method. The column was first packed with approximately 0.5 cm of Magic C4 resin (5 μm, 100 Å, Michrom Bioresources) followed by approximately 20 cm of Maccel C18 AQ resin (3 μm, 200 Å, Nest Group). The total LC-MS/MS run length for each sample was 95 minutes and this comprised a 65 min gradient from 3% to 33% acetonitrile in 0.125% formic acid. Data was collected in data-dependent mode using a TOP20 strategy (Haas et al., 2006) where in each cycle, one full high resolution MS scan in the Orbitrap was followed by up to 20 MS/MS scans in the LTQ for the most intense ions. Collision induced dissociation was used for fragmentation. The MS data was searched using the Sequest search algorithm (Eng et al., 1994). Database searching matched MS/MS spectra with fully tryptic peptides from this database assuming a 50 ppm precursor ion and a product ion tolerance of 0.8 Da. Pupylation of lysine residues (+71.04 Da), acrylamidation of cysteine residues (+71.04 Da) and oxidation of methionine residues (+15.99) were set as variable modifications. Protein hits were filtered at the peptide and protein level to contain fewer than 1% false positives, estimated by the number of decoy hits using in-house software using linear discriminate analysis based on X_{corr}, ΔCn, precursor mass error and charge state, as described previously (Huttlin et al., 2010).

M. tuberculosis supernatant and intracellular cytokinin measurements

Lyophilized supernatants were extracted in Bieleski buffer (60% methanol, 25% $CHCl_3$, 10% HCOOH and 5% H2O) containing a cocktail of internal standards labeled with deuterium, ^{15}N and ^{13}C (each at 1 or 5 pmol per sample; Olchemim). The samples were incubated at 4°C with continuous shaking, centrifuged (15 min, 20000 rpm at 4°C), divided in two, and then purified by a two-step solid phase extraction (SPE) method. In one half, isoprenoid and aromatic cytokinins (bases, ribosides, *N*/*O*-glucosides and nucleotides) were isolated using a combination of silica-based (C18, 500 mg/ 6 mL, Applied Separations, Allentown, PA) and cation-exchange (SCX, 1 g/ 6 mL, Agilent Technologies, Santa Clara, CA) sorbents (Novak et al., 2003). After SPE purification, eluates were evaporated to dryness and dissolved in 20 μl of mobile phase prior to mass analysis using a UPLC Acquity System linked to a Xevo TQ MS spectrometer (Waters Corp., Milford, MA) as described (Svacinova et al., 2012). The second half of the supernatant was purified on 500 mg C18 columns followed by cartridges with 1 ml of DEAE-Sephadex (Sigma-Aldrich, St. Louis, MO) in conjunction with Sep-Pak C18 cartridges (Waters) (Tarkowski et al., 2010). The evaporated samples were dissolved in 20 μl, injected onto a reversed-phase column (Jupiter 5μm C4, 150 mm × 2.0 mm; Phenomenex, Torrace, CA), and eluted with a linear gradient (0 min, 2% B; 0-25 min, 5% B; 25-45 min, 15% B; 25-52 min, 55% B; flow-rate of 0.3 mL/min; column temperature of 30°C) of 20 mM ammonium formate (pH 5.0, A) and acetonitrile (B). 2-methylthio-derivatives of isoprenoid cytokinins in lyophilized culture supernatants were analyzed by LC-MS/MS system (Waters) as described previously (Tarkowski et al., 2010). All chromatograms were analyzed using MassLynx software version 4.1 (Waters), and the compounds were quantified by standard isotope dilution analysis.

Nitrite treatment of *M. smegmatis* and *E. coli*

M. smegmatis nitrite resistance was quantified as for *M. tuberculosis* (Darwin et al., 2003), with except we used a higher concentration of $NaNO_2$ (9 mM versus 3 mM). *E. coli* nitrite sensitivity was tested with an adaptation of previously described protocols (Bower and Mulvey, 2006; Darwin et al., 2003) on strain MG1655. Briefly, overnight cultures of *E. coli* were washed and cell aggregates were removed by low-speed centrifugation. Cultures were diluted to OD_{600} 0.08 into 100 mM MES-buffered LB (pH 5) and exposed to sodium nitrite in 96-well plates. OD_{600} were taken after 24 hours to measure for growth.

RNA extraction and qRTPCR analysis

RNA was extracted from *M. tuberculosis* as previously described (Festa et al., 2010). The Reverse Transcription System (Promega) was used to synthesize cDNA from 100 ng of purified RNA template. The cDNA equivalent of 1.9 ng of RNA was analyzed by qRTPCR using Platinum SYBR GREEN qPCR SuperMIx UDG (Invitrogen) in a MyIQ2 two-color real-time PCR detection system (Bio-Rad), (for primers see Table S1). Analysis was performed using the MyIQ2 software. Normalization was carried out using a standard curve with genomic DNA of known copy number. For quantification, transcript copy numbers were determined by comparison to a standard curve of *M. tuberculosis* genomic DNA. The relative amounts of each transcript were normalized to that of *rpoB*, a control gene that is not differentially regulated in any of our *M. tuberculosis* strains and *dlaT* was used as a negative control (Festa et al., 2011; Pearce et al., 2006).

Cytokinin oxidase activity assay

Wt *M. tuberculosis* cultures were grown to stationary phase, harvested and washed in PBS-Tween (0.05%). Cells were resupended in 0.1 M Tris/HCl, pH 8.5 (30 OD_{580} cell equivalents) and lysed by bead beating with zirconia beads three times for 30 s. Cell lysates were clarified by centrifugation and sterilized through 0.45 μm syringe filters. The reaction mixture containing 0.2 ml cell lysate, 0.5 mM *p*-topolin, 0.15 mM flavin adenine dinucleotide (FAD, Sigma) was incubated at 37°C for 50 min. The reaction was stopped with 0.1 ml 40% trichloroacetic acid. The mixture was centrifuged at 12,000 *g* for 5 min. After addition of 67 μl of 2% 4-aminophenol solution (in 6% trichloroacetic acid), the spectrum over the range 300-600 nm was measured on a SpectraMax M5 spectrophotometer (Molecular Devices) against a blank that included all reagents except the substrate in a UV transparent 96-well plate (Costar). SoftMax Pro (Molecular Devices) was used to record the data. As a control, *p*HBA (final 300 μM) was added to clarified lysate with FAD to confirm the wavelength at which *p*HBA is detected.

Supplemental references:

Ausubel, F.M. (2002). Short protocols in molecular biology: a compendium of methods from Current protocols in molecular biology (New York: Wiley).

Bardarov, S., Bardarov Jr, S., Jr., Pavelka Jr, M.S., Jr., Sambandamurthy, V., Larsen, M., Tufariello, J., Chan, J., Hatfull, G., and Jacobs Jr, W.R., Jr. (2002). Specialized transduction: an efficient method for generating marked and unmarked targeted gene disruptions in *Mycobacterium tuberculosis*, *M. bovis* BCG and *M. smegmatis*. Microbiology *148*, 3007-3017.

Bower, J.M., and Mulvey, M.A. (2006). Polyamine-mediated resistance of uropathogenic *Escherichia coli* to nitrosative stress. J Bacteriol *188*, 928-933.

Burns, K.E., McAllister, F.E., Schwerdtfeger, C., Mintseris, J., Cerda-Maira, F., Noens, E.E., Wilmanns, M., Hubbard, S.R., Melandri, F., Ovaa, H., *et al*. (2012). *Mycobacterium tuberculosis* prokaryotic ubiquitin-like protein-deconjugating enzyme is an unusual aspartate amidase. J Biol Chem *287*, 37522-37529.

Chong, Y.H., Jung, J.M., Choi, W., Park, C.W., Choi, K.S., and Suh, Y.H. (1994). Bacterial expression, purification of full length and carboxyl terminal fragment of Alzheimer amyloid precursor protein and their proteolytic processing by thrombin. Life Sci *54*, 1259-1268.

Darwin, K.H., Lin, G., Chen, Z., Li, H., and Nathan, C.F. (2005). Characterization of a *Mycobacterium tuberculosis* proteasomal ATPase homologue. Mol Microbiol *55*, 561-571.

Datsenko, K.A., and Wanner, B.L. (2000). One-step inactivation of chromosomal genes in *Escherichia coli* K-12 using PCR products. Proc Natl Acad Sci USA *97*, 6640-6645.

Eng, J.K., McCormack, A.L., and Yates, J.R. (1994). An approach to correlate tandem mass spectral data of peptides with amino acid sequences in a protein database. J Am Soc Mass Spectrom *5*, 976-989.

Festa, R.A., Pearce, M.J., and Darwin, K.H. (2007). Characterization of the proteasome accessory factor (*paf*) operon in *Mycobacterium tuberculosis*. J Bacteriol *189*, 3044-3050.

Finn, R.D., Mistry, J., Tate, J., Coggill, P., Heger, A., Pollington, J.E., Gavin, O.L., Gunasekaran, P., Ceric, G., Forslund, K., *et al*. (2010). The Pfam protein families database. Nucleic Acids Res *38*, D211-222.

Haas, W., Faherty, B.K., Gerber, S.A., Elias, J.E., Beausoleil, S.A., Bakalarski, C.E., Li, X., Villen, J., and Gygi, S.P. (2006). Optimization and use of peptide mass measurement accuracy in shotgun proteomics. Mol Cell Proteomics *5*, 1326-1337.

Hatfull, G.F., and Jacobs, W.R.J. (2000). Molecular Genetics of Mycobacteria (Washington, DC: ASM Press).

Horton, R.M. (1997). In vitro recombination and mutagenesis of DNA. SOEing together tailor-made genes. Methods Mol Biol *67*, 141-149.

Huttlin, E.L., Jedrychowski, M.P., Elias, J.E., Goswami, T., Rad, R., Beausoleil, S.A., Villen, J., Haas, W., Sowa, M.E., and Gygi, S.P. (2010). A tissue-specific atlas of mouse protein phosphorylation and expression. Cell *143*, 1174-1189.

Lassmann, T., Frings, O., and Sonnhammer, E.L. (2009). Kalign2: high-performance multiple alignment of protein and nucleotide sequences allowing external features. Nucleic Acids Res *37*, 858-865.

Pearce, M.J., Arora, P., Festa, R.A., Butler-Wu, S.M., Gokhale, R.S., and Darwin, K.H. (2006). Identification of substrates of the *Mycobacterium tuberculosi*s proteasome. EMBO J *25*, 5423-5432.

Price, M.N., Dehal, P.S., and Arkin, A.P. (2010). FastTree 2--approximately maximum-likelihood trees for large alignments. PLoS One *5*, e9490.
Rappsilber, J., Ishihama, Y., and Mann, M. (2003). Stop and go extraction tips for matrix-assisted laser desorption/ionization, nanoelectrospray, and LC/MS sample pretreatment in proteomics. Anal Chem *75*, 663-670.
Sambrook, J., Maniatis, T., and Fritsch, E. (1989). Molecular Cloning: A Laboratory Manual. (Cold Spring Harbor: Cold Spring Harbor Laboratory Press.).
Snapper, S.B., Melton, R.E., Mustafa, S., Kieser, T., and Jacobs, W.R., Jr. (1990). Isolation and characterization of efficient plasmid transformation mutants of *Mycobacterium smegmatis*. Mol Microbiol *4*, 1911-1919.
Stover, C.K., de la Cruz, V.F., Fuerst, T.R., Burlein, J.E., Benson, L.A., Bennett, L.T., Bansal, G.P., Young, J.F., Lee, M.H., Hatfull, G.F., *et al*. (1991). New use of BCG for recombinant vaccines. Nature *351*, 456-460.
Tian, J., Bryk, R., Itoh, M., Suematsu, M., and Nathan, C. (2005). Variant tricarboxylic acid cycle in *Mycobacterium tuberculosis*: identification of alpha-ketoglutarate decarboxylase. Proc Natl Acad Sci USA *102*, 10670-10675.
van Helden, P.D., Victor, T.C., Warren, R.M., and van Helden, E.G. (2001). Isolation of DNA from *Mycobacterium tubercolosis*. Methods Mol Med *54*, 19-30.